Elsevier required licence: © 2019

This manuscript version is made available under the
CC-BY-NC-ND 4.0 license

http://creativecommons.org/licenses/by-nc-nd/4.0/

The definitive publisher version is available online at

https://doi.org/10.1016/j.chemosphere.2019.02.033

Declaration of interest: None

Simultaneous removal of polycyclic aromatic hydrocarbons and heavy metals from water using granular activated carbon

Dinushika Eeshwarasinghe, Paripurnanda Loganathan, Saravanamuthu Vigneswaran*

Faculty of Engineering, University of Technology Sydney (UTS), P.O. Box 123, Broadway, NSW 2007, Australia

**Corresponding author. Tel.:+61 2 95142641, fax: +61 2 95142633.*

Email: s.vigneswaran@uts.edu.au

Highlights

- GAC adsorption of polycyclic aromatic hydrocarbon (PAH) higher than heavy metals.
- PAHs' adsorption capacities reduced by heavy metals in the order, Cu > Zn > Cd.
- GAC's negative zeta potential reduced by adsorption of heavy metals: Cu > Zn > Cd.
- Intra-particle diffusion of heavy metals and PAHs into GAC's meso and micro pores.
- Langmuir adsorption capacity of phenanthrene (higher log Kow)) > acenaphthylene.

Abstract

Polycyclic aromatic hydrocarbons (PAHs) and heavy metals are dangerous pollutants that commonly co-occur in water. An adsorption study conducted on the simultaneous removal of

PAHs (acenaphthylene, phenanthrene) and heavy metals (Cd, Cu, Zn) by granular activated carbon (GAC) showed that, when these pollutants are present together, their adsorption was less than when they were present individually. The adsorptive removal percentage of PAHs (initial concentration 1 mg/L) was much higher than that of heavy metals (initial concentration (20 mg/L). The reduction in adsorption of PAHs by heavy metals followed the heavy metals' adsorption capacity and reduction in the negative zeta potential of GAC order (Cu > Zn > Cd). In contrast, PAHs had little effect on the zeta potential of GAC. The Langmuir adsorption capacities of acenaphthylene (0.31-2.63 mg/g) and phenanthrene (0.74-7.36 mg/g) on GAC decreased with increased metals' concentration with the reduction following the order of the metals' adsorption capacity. The kinetic adsorption data fitted to Weber and Morris plots, indicating intra-particle diffusion of both PAHs and heavy metals into the mesopores and micropores in GAC with the diffusion rates. This depended on the type of PAH and metal and whether the pollutants were present alone or together.

Keywords: heavy metals, polycyclic aromatic hydrocarbon, adsorption, zeta potential, water treatment

1. Introduction

Elevated concentrations of heavy metals and polycyclic aromatic hydrocarbons (PAHs) are known to have adverse effects on the aquatic environment due to their high toxicity and long persistence. They can be potentially carcinogenic, mutagenic or allergenic to humans and furthermore produce many other toxicity outcomes when they enter via the aquatic food chain [1-6]. They are very commonly found to occur together and their combined toxicity is reported to be higher than their individual toxicities [7].

Several treatment methods have been used to remove these pollutants from water such as ion exchange /adsorption, biodegradation, photocatalysis oxidation, chemical precipitation, membrane filtration, and electrochemical techniques [1,4,5,8-11]. Of these, adsorption is the most cost-effective, simple, flexible and efficient process. As well, it produces minimum chemical or biological sludge and the adsorbent can be regenerated and reused which leads to a more cost-effective process.

Numerous studies have been reported on the adsorptive removal of heavy metals [1,8,9] and PAHs [10-13] but very few of these have dealt with the simultaneous removal of both of these pollutants. Simultaneous removal is important because PAHs' and heavy metals' co-occurrence is very common in the environment, especially when the water contains both industrial and domestic waste discharges [14] and in stormwaters containing road-deposited sediments [15,16]. Considering the importance of the simultaneous removal of these pollutants, in recent times more focus has been directed on conducting research on this topic.

Studies have reported both competitive and synergistic effects on the adsorption of PAHs and heavy metals. Chen et al. [17] found that the presence of Cu decreased the adsorption of naphthalene by wood black carbon and explained this outcome as due to surface complexation of Cu to form hydration shells of dense water that competed with naphthalene for adsorption. They also stated that pore blockage by the hydrated Cu inhibited naphthalene adsorption. Huang et al. [18] compared the individual and combined adsorption capacities of Cd and acenaphthene on a maghemite/mesoporous silica composite. They found that the adsorption capacities decreased from those of individual capacities when acenaphthene and Cd were present together. The competitive effect had a higher impact on Cd adsorption than on acenaphthene adsorption. Also, Huang et al. [18] explained this as due to faster adsorption of acenaphthene which allowed it to occupy the adsorption sites first rather than Cd. In a study on the adsorption of Pb and pyrene in a soil, Pb curtailed the adsorption of pyrene and pyrene reduced the adsorption of Pb due to competitive adsorption [19].

In contrast to the competitive effects, synergistic effects of heavy metals and PAHs have also been reported in some studies. For example, Zhang et al. [20] found that Cu and pyrene adsorption capacities on Fe functionalised mesoporous silica were higher when they were present together than when they were present alone. They explained this observation as due to the formation of a Cu-pyrene complex through cation-π interaction (non-covalent binding force between metals and aromatic organic compounds) where the complex had stronger affinity to the adsorbent than the individual components. Formation of pyrene-Cu bridging was also suggested for the mutual promotion of the adsorption. The higher adsorption of PAHs (acenaphthene, fluorene and fluoranthene) and heavy metals (Ni, Pb, Zn) when they are present together compared to their individual presence was also reported for adsorption on clay minerals [21]. This was explained as due to the formation of a cation-π bond with the effect being greater for the higher molecular weight PAHs. The reason for this was the larger number of benzene rings providing more electrons for π-interaction. Tao et al. [14,22] studied the effects of various metals on the adsorption of selected PAHs by aquatic dead phytoplankton biomass and reported that a change in the concentration of the metals had different effects on the adsorption behaviour of the PAHs. Sorption enhancement which occurred at medium metal concentrations, was reportedly caused by these cation- π interactions, and increased with the order of softness of the metals, and the π-donor strength of the PAHs.

Simultaneous adsorption of PAHs and heavy metals has not been studied in detail on activated carbon (AC) adsorbent, which is one of the most popular and reliable adsorbents used for removing both heavy metals [14,23-25] and PAHs [11-13,26]. Inner-sphere complexation of heavy metals adsorption on AC has been established in previous studies using zeta potential data [24] and this might have relevance to the simultaneous adsorption of PAHs and heavy metals on AC. We have also shown earlier that the porosity of granular AC (GAC) did influence PAH adsorption kinetics [12], which could in turn have an impact on the mutual adsorption of PAH and heavy metals. These aspects will be used to explain the simultaneous adsorption of heavy metals having different affinities to GAC and PAHs in the study presented here. The aims of the study, therefore, were to: firstly, determine the effects of different concentrations of Cu, Cd, and Zn on the equilibrium and kinetics of acenaphthylene and phenanthrene adsorption on GAC; secondly, determine the effect of these two PAHs on the equilibrium and kinetics of adsorption of the three heavy metals; thirdly, explain the mechanism of adsorption using zeta potential data; and fourthly, model the adsorption behaviour of the heavy metals and PAHs when they occur separately and together. Such modelling has not been previously reported for simultaneous adsorption of PAHs and heavy metals.

2. Materials and methods

2.1. Materials

GAC (0.3–2.4 mm) for this study was purchased from James Cummins P/L, Australia. A particle size range of 400-800 µm was separated from the original material and used in the experiments. The BET surface area, pore volume and average pore diameter of the GAC were 1010 m^2/g, 0.69 cm^3/g and 2.7 nm, respectively [12]. The scanning electron micrographs of the GAC (Fig. 1) revealed the presence of large numbers of micropores and mesopores which may have resulted in GAC having high surface area.

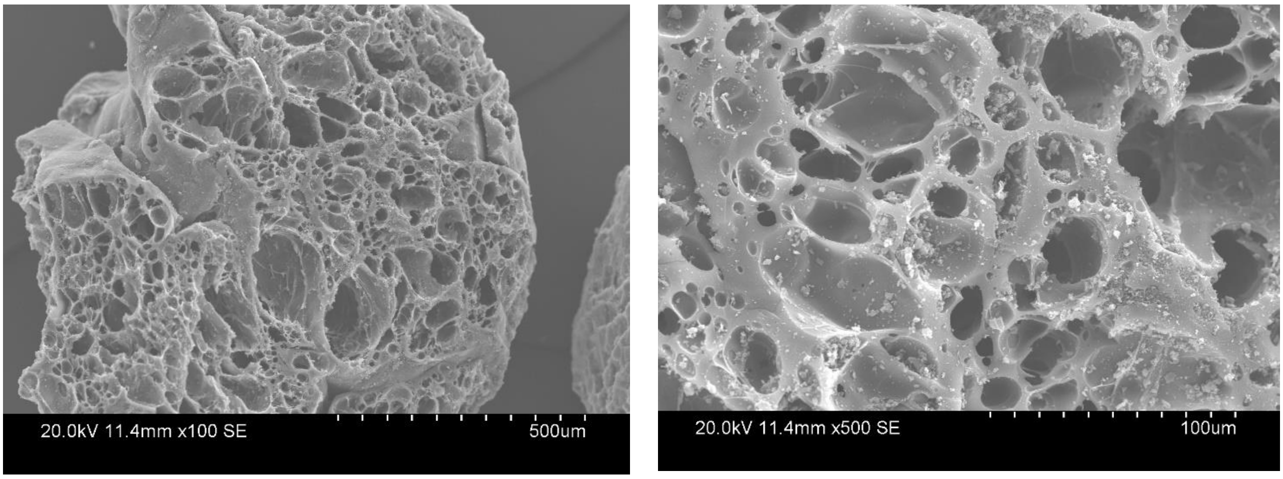

Fig. 1. Scanning electron micrographs of GAC [12].

The PAHs used in the study were acenaphthylene ($C_{12}H_8$, $\log K_{ow}$ 3.94, molar volume 168 cm^3/mol) and phenanthrene ($C_{14}H_{10}$, $\log K_{ow}$ 4.46, molar volume 199 cm^3/mol) [12]. As the PAHs were only partially soluble in water, their solutions were prepared from concentrated stock solutions of each PAH dissolved in acetonitrile. The stock solutions contained 20 mg PAH in 20 mL acetonitrile (1 g/L). Solutions employed for the studies were prepared by diluting the stock solutions in 1% acetonitrile in Milli-Q® water. Acetonitrile and PAHs used were spectroscopic grade materials purchased from Sigma-Aldrich, USA. Heavy metals studied were Cu, Cd and Zn. Analytical grade (99% purity) nitrate salts of these metals were employed in the experiments to prepare the heavy metals solution. These salts were also purchased from Sigma-Aldrich (USA).

2.2. Chemical analysis

PAH concentration in the solution was determined using UV–VIS Spectrophotometry (Shimadzu UV-1700). The absorbance values of acenaphthylene and phenanthrene were determined at the wavelengths of 321 nm and 226 nm, respectively. These wavelengths proved to be the optimum values for measuring the concentrations of these PAHs, both in the presence and absence of heavy metals (Figs. S1, S3-S6, supplementary data). These PAHs' concentrations were determined from standard curves of absorption vs concentrations of the standards (Figs. S2, S7, S8). The glassware used in the experiments were initially washed and rinsed with deionised water and then soaked overnight in dilute nitric acid bath before use. PAH losses caused by photodegradation were minimised by covering all flasks containing PAH solutions with aluminium foil. The flasks were also tightly sealed to prevent any losses occurring through volatilisation. Heavy metal concentrations were determined using a Microwave Plasma-Atomic Emission Spectrometer (Agilent 4100 MP-AES).

2.3. Zeta potential

The zeta potential of GAC was conducted in the presence of 10^{-3} M of $NaNO_3$ at pH levels of 4, 5, and 6 with and without additions of heavy metals and PAHs using a Zetasizer nano instrument (Nano ZS Zen3600, Malvern, UK). 10^{-3} M of $NaNO_3$ was used to keep the ionic strength of all solutions constant. The concentrations of GAC (< 0.075 mm particle size), heavy metals, and PAHs in the suspensions were 0.6 g/L, 20 mg/L, and 1 mg/L, respectively. The measurements were made after the suspensions were agitated in a flat shaker at a speed of 120 rpm for 22 h. As the pH level changed from the initial pH during PAHs and heavy metals adsorption, the pH levels were adjusted back to the initial pH after 3 h of shaking. pH adjustments were made by adding diluted HCl or NaOH. The initial pH, pH after 3 h and the final pH were measured using a pH meter.

2.4. Adsorption experiments

A series of glass flasks containing 70 mL solutions at pH 5 in the presence of PAHs and heavy metals together or individually were agitated with different GAC doses ranging from 0.05 to 0.8 g/L in a flat shaker at 120 rpm for 5 h at room temperature (24 ± 1 °C). The concentration of PAHs was 1 mg/L whereas that of heavy metals was 5, 20 or 50 mg/L. Much higher concentrations were used for heavy metals to be in consistent with the difference in concentrations between PAHs and heavy metals found in industrial and domestic wastewaters where the concentrations of heavy metals are 10-1000 times those of PAHs [6,27,28]. All solutions contained 0.005 M $NaNO_3$ to ensure the ionic strength remained constant. The suspensions were then filtered and subsequently the filtrates were analysed for PAHs and heavy metals. The amount of PAH and heavy metal adsorption at equilibrium, q_e (mg/g), was calculated using the equation given below:

$$q_e = \frac{(C_0 - C_e).V}{M}$$

where, C_0 is initial concentration of PAH or heavy metal (mg/L), C_e is equilibrium concentration of PAH or heavy metal (mg/L), V is volume of solution (L) and M is mass of adsorbent (g). Percentage adsorption was calculated using the following equation and the data were fitted to the mathematical models described in Table 1:

$$\text{Percentage adsorption (\%)} = \frac{(C_0 - C_e)}{C_0} \text{ x } 100$$

The kinetics of adsorption was conducted at pH 5 in the presence of 0.005 M $NaNO_3$ with an adsorbent dose of 0.3 g/L, PAHs concentration of 1 mg/L, and heavy metals concentration of 20 mg/L, by shaking the suspensions at 120 rpm in a flat shaker at room temperature. Samples were taken at different periods of time (10 min – 24 h), and after filtration of the suspensions, the filtrates were analysed for PAHs and heavy metals. The amount of PAH or heavy metal adsorption (q_t) at time t was estimated as described below:

$$q_t = \frac{(C_0 - C_t)V}{M}$$

where, C_0 is initial concentration of PAH or heavy metal (mg/L), C_t is concentration of PAH or heavy metal at time t (mg/L), V is volume of the solution (L) and M is mass of adsorbent (g). Both the equilibrium and kinetic adsorption data were fitted to the mathematical models presented in Table 1.

Table 1. Adsorption models used in the study

Model	Equation
Equilibrium models	
Langmuir[1,2]	$q_e = \frac{q_m K_L C_e}{1 + K_L C_e}$ C_e = equilibrium concentration of PAH or heavy metals (mg/L), q = amount of PAH adsorbed per unit mass of adsorbent (mg/g), q_m = maximum amount of PAH or heavy metals adsorbed per unit mass of adsorbent (mg/g), K_L = Langmuir constant (L/mg) relates the energy of adsorption
Freundlich[1,2]	$q_e = K_f C_e^{1/n}$ k_f = Freundlich constant (mg/g) (L/mg)$^{1/n}$, n = Freundlich constant, q_e = the amount adsorbed per unit dosage of the adsorbent (mg/g)
Dubinin–Radushkevich[3,4]	$\ln(q_e) = \ln(q_m) - \beta\varepsilon^2$ q_m = the monolayer capacity, β = the activity coefficient related to mean adsorption energy and ε = Palanyi potential described as: $\varepsilon = RTln[1 + \frac{1}{C_e}]$ where R = universal gas constant 8.314 (J/mol.K), T = absolute temperature (K), From the plots of $\ln(q_e)$ versus ε^2 the values of β and q_m were determined
Kinetic models	
Pseudo-first order [1,2]	$\frac{dq_t}{dt} = k_1(q_e - q_t)$ q_e = amount of PAH or heavy metals adsorbed at equilibrium (mg/g), q_t = amount of PAH or heavy metals adsorbed at time t (h), (mg/g), k_1 = rate constant for pseudo-first order adsorption (1/h)
Pseudo-second order[1,2]	$\frac{dq_t}{dt} = k_2(q_e - q_t)^2$ k_2 = rate constant for pseudo-second order adsorption (g/mg.h)
Weber and Morris[3,5]	$q_t = K_p t^{1/2} + B$ k_p = intra-particle diffusion rate constant (mg/(g.h$^{1/2}$)), B = constant which provides a measure of the boundary layer thickness (mg/g)

[1] Ahmanuzzaman [1]; [2] Kalaruban et al. [29];]; [3]Eeshwarasinghe et al. [12]; [4]Alade et al. [26];

[5]Weber and Morris [30],

3. Results and discussion

3.1. Equilibrium adsorption

The adsorptive removals of PAHs in the presence and absence of heavy metals are shown as percentage removal of initially added PAHs for the initial PAHs concentration of 1 mg/L and heavy metals concentration of 20 mg/L in Fig. 2. For comparative purposes the percentage of removal of heavy metals alone and in the presence of PAHs are also shown in the same figure as well as in Fig. 3 where the results are illustrated more clearly by expanding the Y-axis scale. Similar results are presented in Fig. S9 (supplementary data) for the initial PAHs concentration of 1 mg/L and heavy metals concentration of 5 mg/L. The data show that the percentages of PAHs removed are many times higher than those of the heavy metals despite the latter having 20 times larger concentrations in solution. This indicates that PAHs have higher affinity to GAC than heavy metals do. This is because the hydrophobic interaction and H-bonding of the PAHs with the hydrophobic GAC surface and functional groups [12,17] are more dominant than the cationic heavy metal ions' exchange/chelation/complexation ability with the limited negatively charged functional groups on GAC [17,24,31]. The removal percentages fell when PAH and heavy metals were present together compared to their respective individual presence (Fig. 2 and 3), indicating there was competition for adsorption between PAHs and heavy metals. The competitive effect of PAHs on heavy metals adsorption is higher than the heavy metals' effect on PAHs adsorption. Enhancement of PAHs adsorption by heavy metals presence reported for other adsorbents due to metal cation - π interaction [20,22] seems to be less important than the competitive adsorption effect in the case of GAC.

Because the percentage removal of PAHs and heavy metals presented in Fig. 2, 4 and S9 depend on their initial concentrations the results are also presented as amounts adsorbed (amounts removed) in Fig. 3, 5, S10 and S11. These figures show that in the case of 20 mg/L of heavy metals the amounts of metals adsorbed are nearly twice those of acenaphthylene, because the heavy metals concentrations were 20 times that of acenaphthylene. For phenanthrene which has a higher affinity to GAC, the amounts adsorbed were nearly the same as the heavy metals. However, when the heavy metals concentrations were reduced to 5 mg/L the amounts adsorbed for both the PAHs were higher than those of heavy metals, indicating that the PAHs have higher affinity than heavy metals towards GAC.

At all GAC doses the adsorptive removal of phenanthrene was higher than that of acenaphthylene, both in the presence and absence of metals. This is probably due to the higher hydrophobicity of the phenanthrene (log K_{ow} 4.46; K_{ow} 28,840) than that of acenaphthylene (log K_{ow} 3.94; K_{ow} 8709), though pH changes during adsorption might have also influenced the hydrophobicity difference between the two PAHs. This is consistent with the findings of other studies which reported that the adsorption capacity of PAHs increased with increasing log K_{ow} [11-13]. Another reason could be the higher number of benzene rings in phenanthrene (3 rings) compared to those in acenaphthylene (2 rings). Ge et al. [32] reported that PAHs' adsorption capacity increased when the number of benzene rings also increased in PAH. This can be explained as being due to increased π-π complex formation between the π-electrons of benzene rings and the active sites on an AC surface.

Generally, the adsorption of PAHs was reduced by the metals in the order of Cu ≥ Zn > Cd which is closely related to the metals' adsorption capacity (Fig. 3). Sounthararajah et al. [33] reported that the adsorption capacities of metals on GAC, both in batch and column experiments, followed the order Cu > Zn > Cd. They explained this as due to Cu having the lowest pK_1 (first hydrolysis constant K_1, highest tendency to form $Cu(OH)^+$) and highest hydroxide precipitate solubility product pK_{so} (metal hydroxide precipitation potential high when pK_{so} is high) and Cd having the highest pK_1 and lowest pK_{so}. Erto et al. [34] also reported similar explanations for the higher adsorption of Zn than Cd. They also stated that

Zn^{2+} being smaller in size than Cd^{2+} was able to penetrate smaller pores in AC and furthermore it was less affected by steric hindrance during adsorption. McBride [35] provided another explanation for the metal affinity order based on ionic potential (Z^2/r) (Z is charge and r is radius of the metal ion) which followed the same order as the affinity. The metals' reaction with the functional groups can also influence the adsorption behaviour. The strength of this reaction is reported to be higher for Cu than Zn [35].

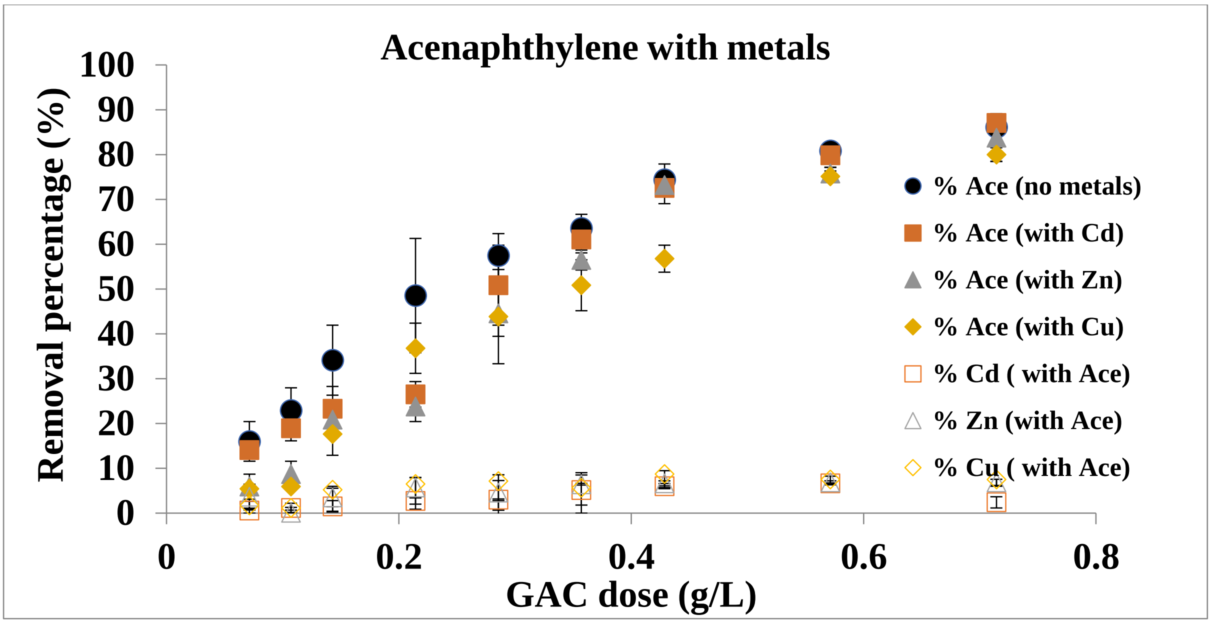

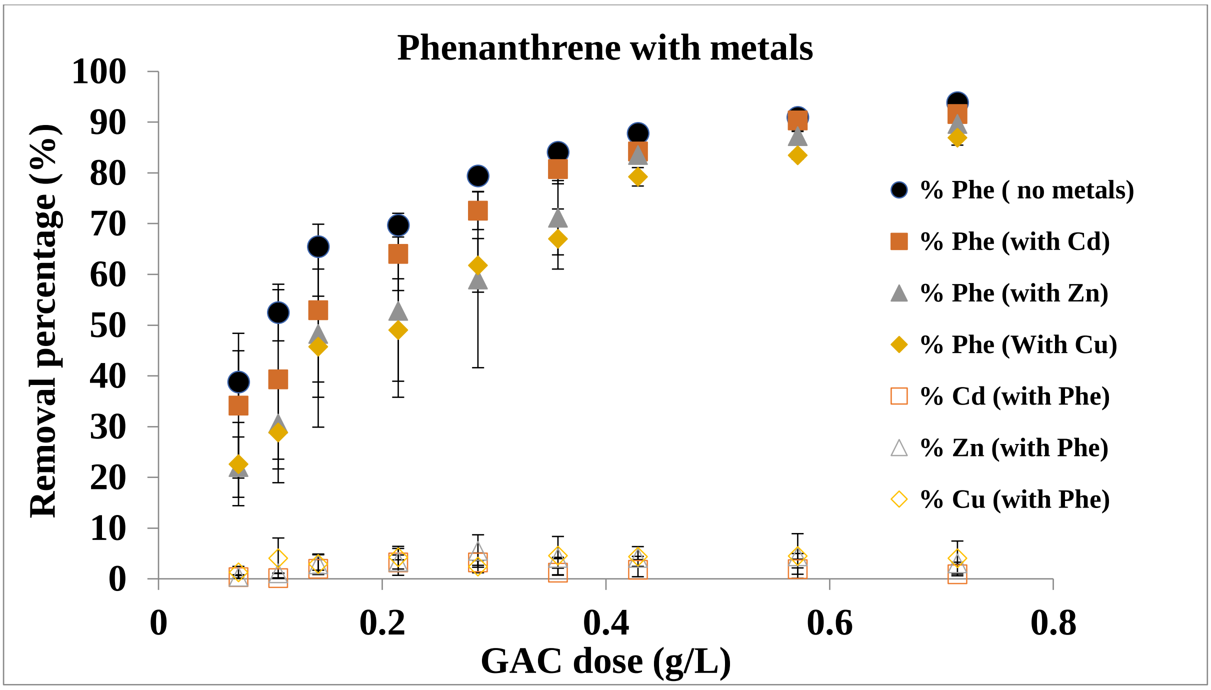

Fig. 2. Percentage removal of acenaphthylene and phenanthrene compared with percentage removal of heavy metals during their simultaneous adsorption on GAC in the presence of 0.005 M $NaNO_3$ (PAH concentration 1 mg/L, metal concentration 20 mg/L).

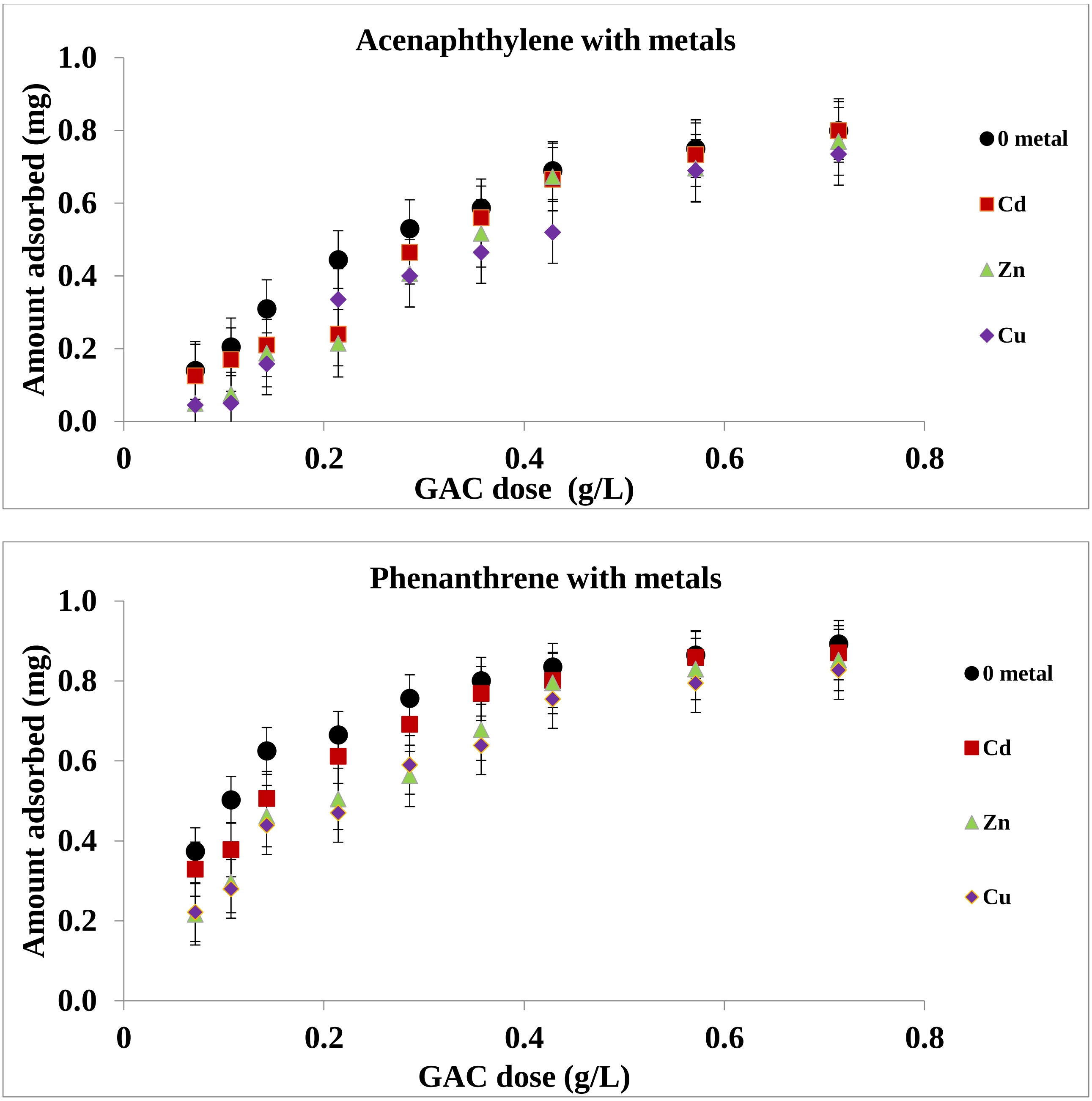

Fig. 3. Amount of acenaphthylene and phenanthrene removed compared with amount of heavy metal removal during their simultaneous adsorption on GAC in the presence of 0.005 M $NaNO_3$ (PAH concentration 1 mg/L, metal concentration 20 mg/L).

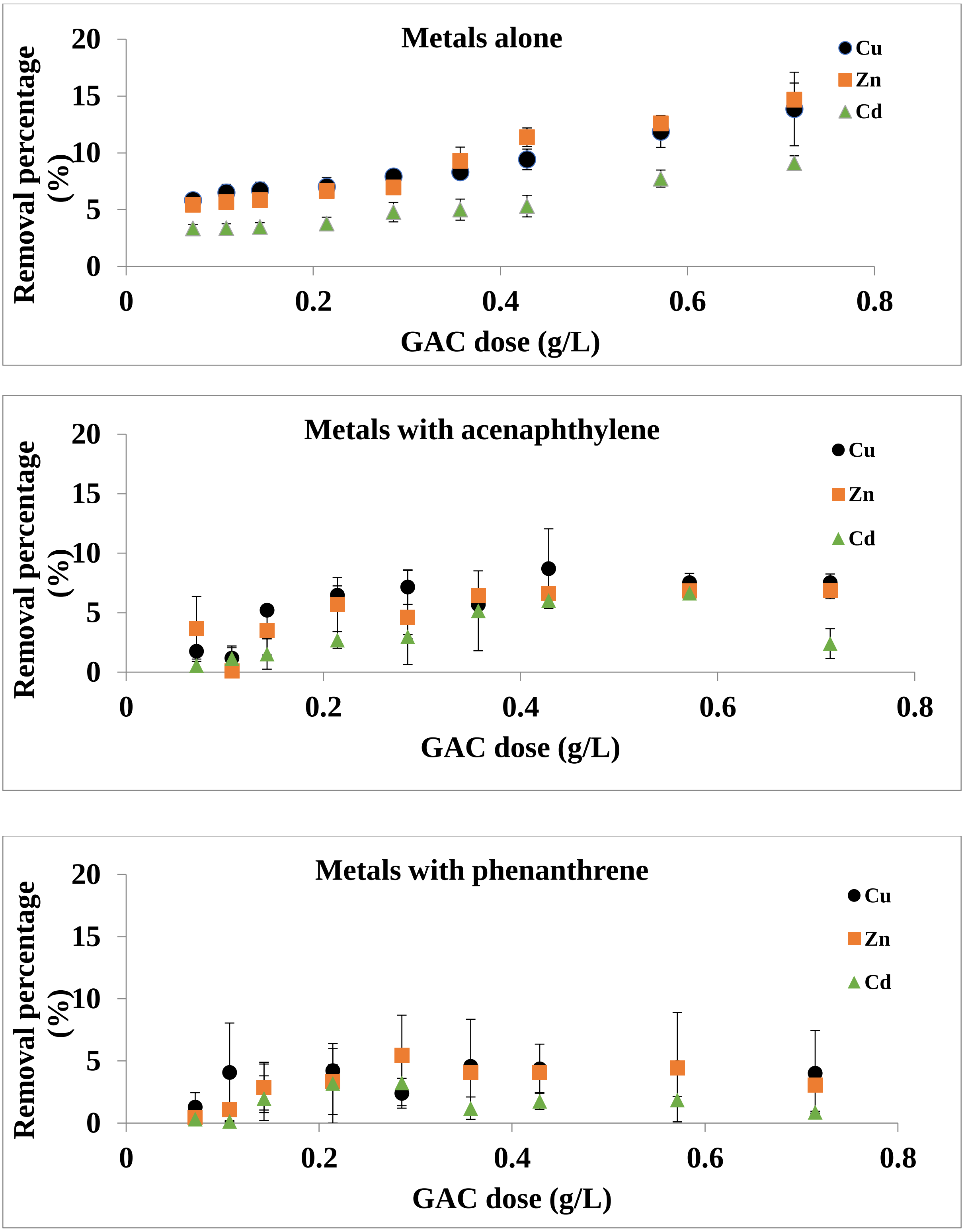

Fig. 4. Percentage removal of heavy metals from solutions with and without the presence of acenaphthylene and phenanthrene (solutions with initial concentrations: 0.005 M $NaNO_3$, PAH 1 mg/L, metal 20 mg/L).

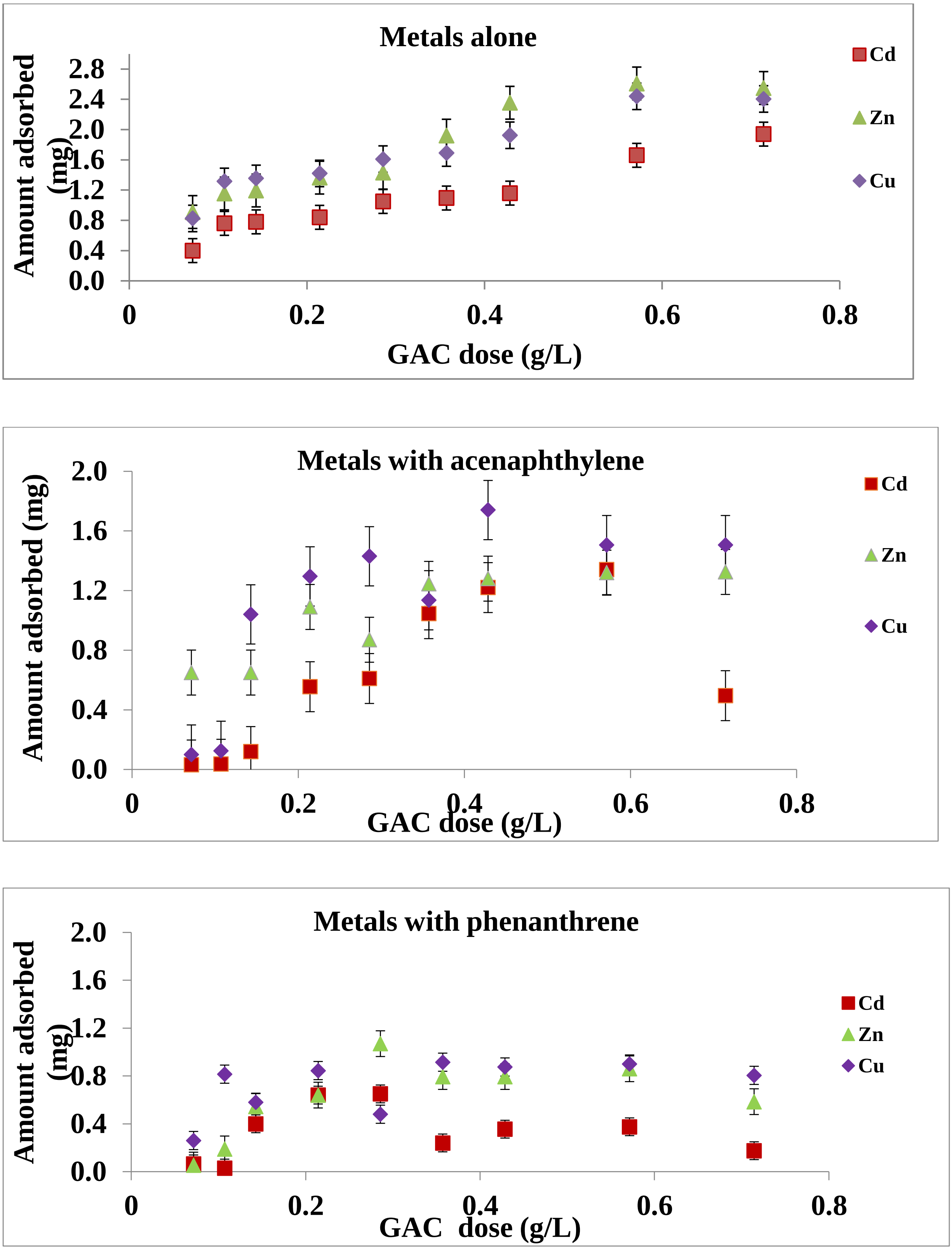

Fig. 5. Amount of heavy metals adsorbed from solutions with and without the presence of acenaphthylene and phenanthrene (solutions with initial concentrations: 0.005 M $NaNO_3$, PAH 1 mg/L, metal 20 mg/L).

3.2.Zeta potential

Since the adsorption of heavy metals is governed by metals' electrostatic interaction with the GAC surface, the zeta potential of GAC which reflects the surface charge, was studied at various pH levels in the presence of heavy metals and PAHs. The negative zeta potential of GAC in the absence of metals had the highest values (Fig. 6 and 7) which favours the adsorption of the positively charged metals and it increased with pH due to increased deprotonation of acidic functional groups. The data showed that the zero point of charge (ZPC, pH at which the net charge is zero) of GAC was 4.2. The low zero point of charge suggests that the GAC surface predominantly comprises -COOH functional groups [36].

The addition of PAHs to GAC suspensions had little effect on the zeta potential because the PAHs had very few charges (Fig. 6 and 7). However, the addition of heavy metals had strong effects on the zeta potential of GAC by drastically reducing the negative surface potential. Addition of Cu reversed the negative zeta potential of GAC to positive values at all pH values and Zn alone or with acenaphthylene either changed the negative potential to zero or to positive values at pH values less than 5.5. The extent of reduction of the negative zeta potential followed the same order of the adsorption capacity of the metals (Cu > Zn > Cd) (Fig. 5). The strong reduction in the negative zeta potential indicates that the metals were adsorbed by inner-sphere complexation (specific adsorption) by exchanging with the protons on the GAC surface functional groups [24]. The possible reasons for the differences between the metals in alteration of the zeta potential were same as the metals' adsorption capacity differences discussed in the earlier section.

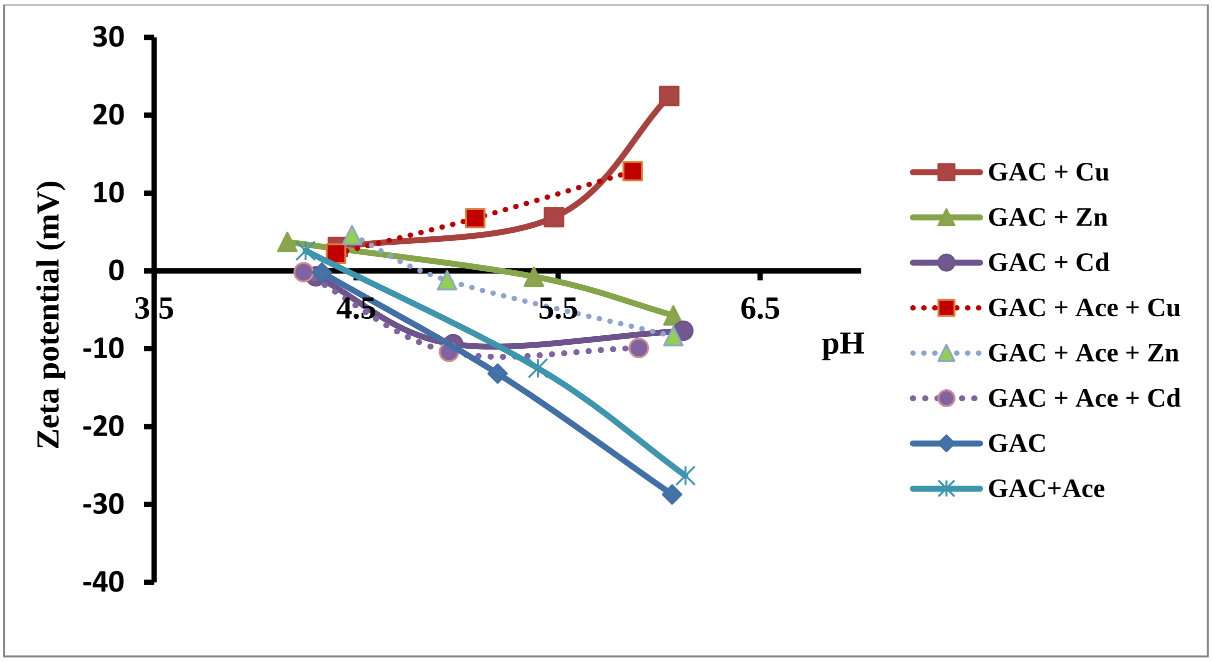

Fig. 6. Effect of pH on the zeta potential of GAC (0.6 g/L) with and without metals (20 mg/L) and acenaphthylene (1 mg/L).

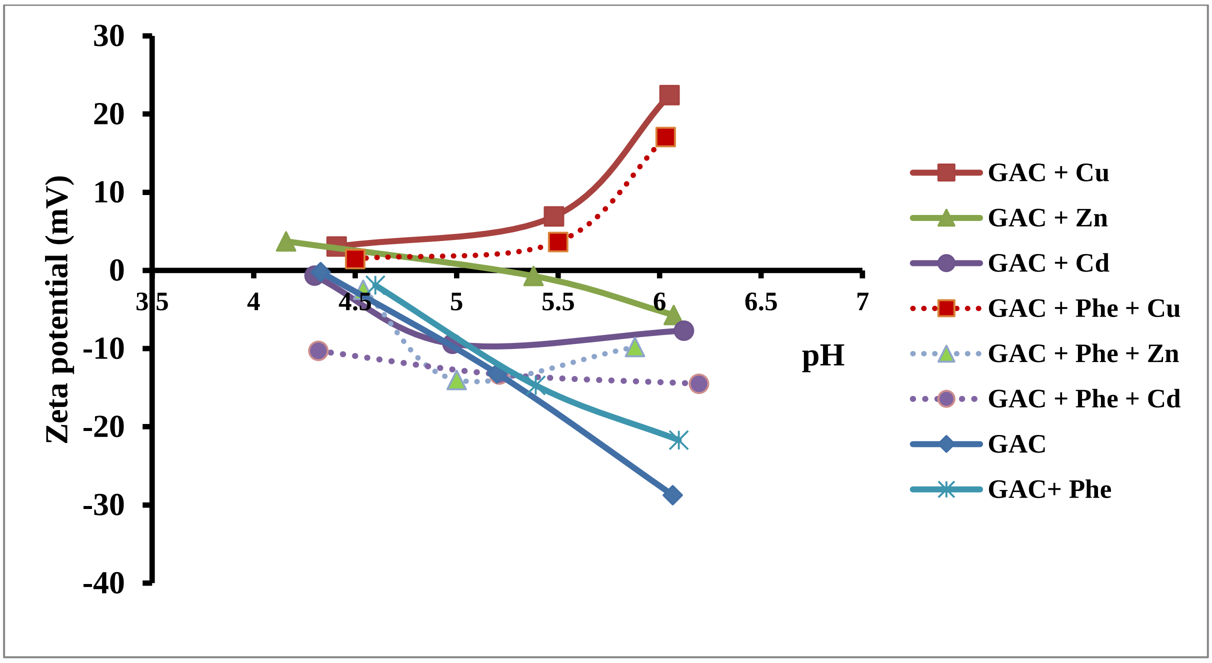

Fig. 7. Effect of pH on the zeta potential of GAC (0.6 g/L) with and without metals (20 mg/L) and phenanthrene (1 mg/L).

3.3. pH changes during adsorption

At all initial pH levels, the pH increased for all treatments (ΔpH positive) (Fig. 8). The ΔpH was highest for the lowest initial pH of 4 because, at this low pH, the protons (H^+) which are at high concentration in solution, adsorb onto the negatively charged sites on GAC. This causes a decrease in their concentration in solution, thus producing a higher pH [36]. However, this increase in pH is lowered when heavy metals are added to the GAC because: firstly, the metals compete with protons for adsorption; and secondly, protons are released to the solution by exchanging with the metals adsorbed [29,37]. In the presence of PAHs, heavy metals adsorption declined due to competition for adsorption with PAHs and therefore the increase in pH remained approximately the same as in the GAC alone treatment except for Cu which has higher adsorption capacity than the other metals even when PAHs are present. Consistent with this data, the zeta potential of GAC was reversed from negative to positive values in the presence of Cu and Cu + PAH (Fig. 6 and 7).

As the initial pH increased, ΔpH was reduced because the adsorption of protons declined due to the presence of lower proton concentration in solution and the higher adsorption of metals releasing more protons [36,37]. This is more striking for Cu than Cd and Zn because Cu was adsorbed in higher quantities.

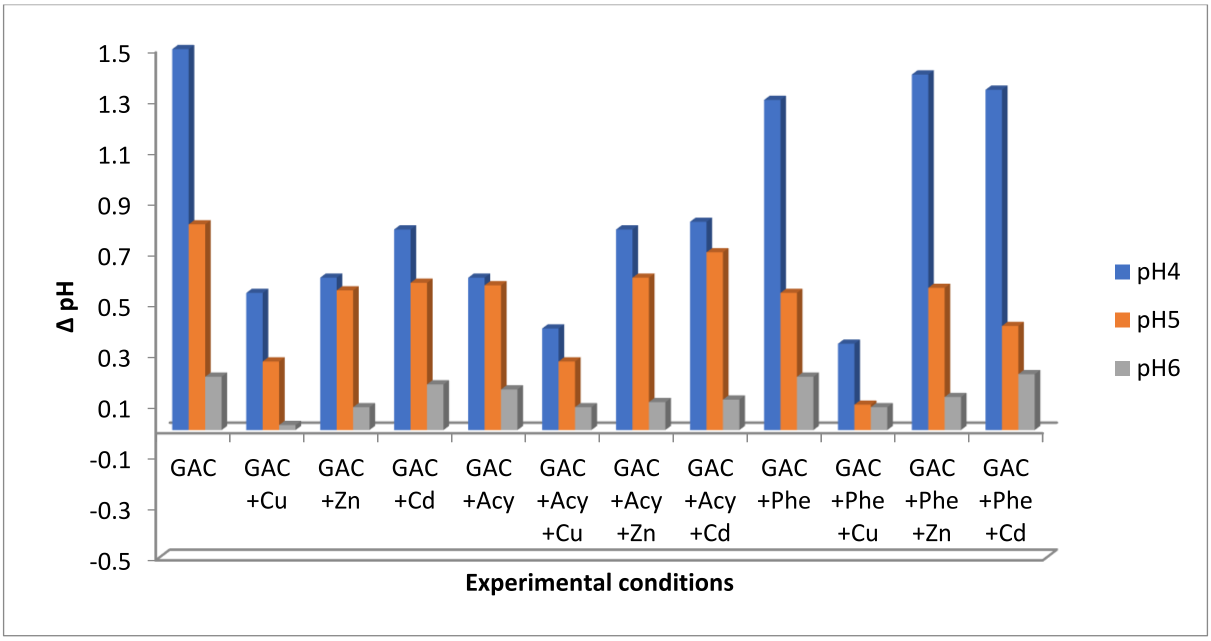

Fig. 8. Effect of initial pH, heavy metal, and PAH on change in pH (ΔpH = final pH – initial pH) during adsorption on GAC.

Fig. 9 shows that there is a negative relationship between ΔpH and Δzeta potential (zeta potential of GAC in the presence of heavy metals with and without PAHs – zeta potential of GAC alone). As the initial pH increased from 4 to 6, Δzeta potential increased because specific adsorption (inner-sphere complexation) of metals, especially Cu and Zn, increased [24]. During the specific adsorption of metals, protons (H^+) are released from the functional groups on the GAC surface. The final pH was thus reduced and ΔpH decreased. At the initial pHs of 5 and 6, Δzeta potential followed the order Cu > Zn > Cd but ΔpH followed the reverse order of Cd ≥ Zn > Cu, regardless of the presence or absence of PAHs.

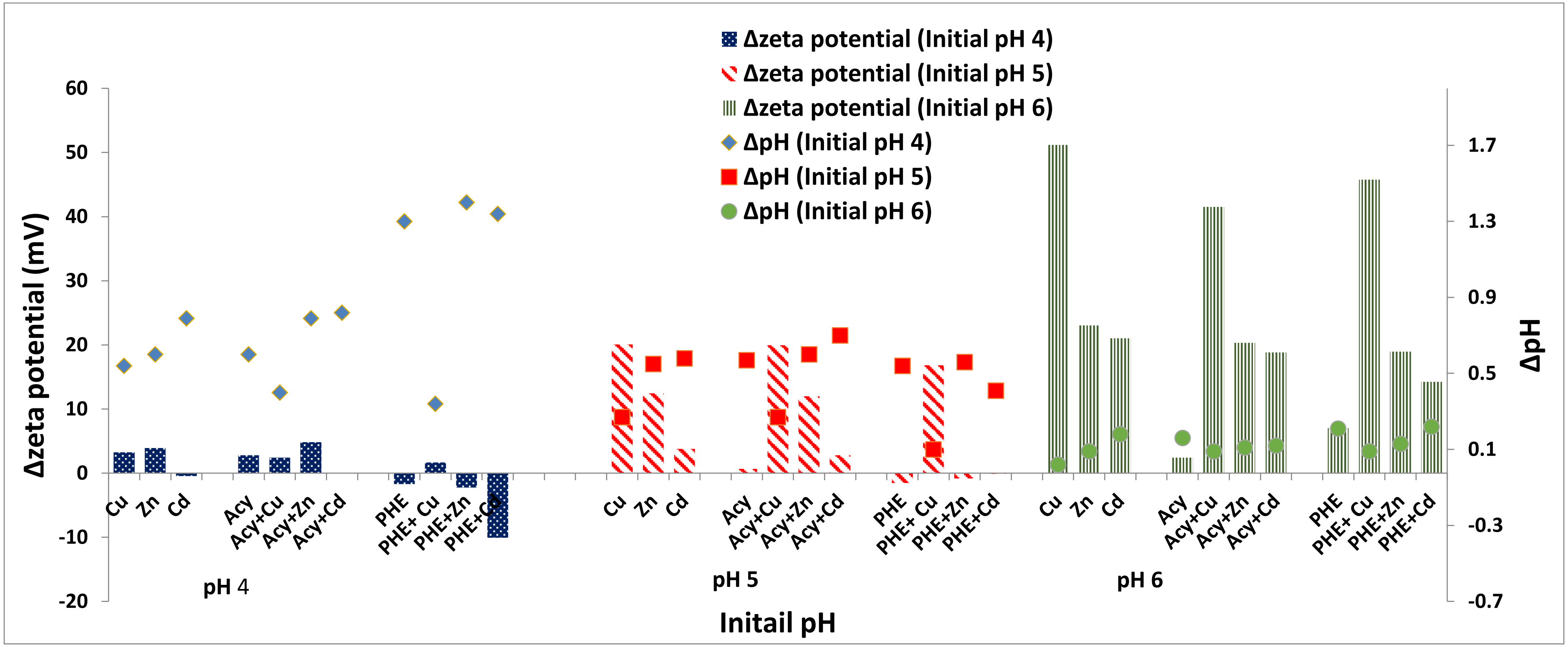

Fig.9 Relationship between ΔpH (Final pH - initial pH) and Δzeta potential (zeta potential of GAC with heavy metals and PAHs – zeta potential of GAC alone) at three initial pHs during adsorption (▩ ▧ ▥ - Δzeta potential; ◆ , ■ and ● - ΔpH)

3.4. Equilibrium adsorption modelling

Three adsorption models, namely Langmuir, Freundlich and Dubinin–Radushkevick models were used to describe the equilibrium adsorption data. Of these models, Langmuir model satisfactorily described the data for both PAHs with and without metals at different concentrations (Tables 3 and 4). The R^2 values ranged from 0.60 to 0.88 for a degree of freedom of data points of 8 (9 data points). This means that the model explained 60-88% of the variation of data. R^2 value > 0.76 (correlation coefficient, r = 0.87) for a degree of freedom of 8 indicates a very highly significant relationship [38]. R^2 value > 0.59 (r = 0.76) indicates a highly significant relationship. Freundlich model fitted well to the data for phenanthrene (Table 4) except for phenanthrene with 50 mg/L concentration of metals. But it failed to satisfactorily describe the data for acenaphthylene. Dubinin–Radushkevick model satisfactorily described the data for both PAHs in the absence of metals but the data fit to this model was poor in the presence of metals at most of the concentrations.

The fairly satisfactory data fit to Langmuir model may indicate that the PAHs were adsorbed as monolayers on the GAC. The Langmuir maximum adsorption capacity of phenanthrene (7.36 mg/g) was higher than that of acenaphthylene (2.63 mg/g) due to the higher hydrophobicity of the former (log K_{ow} 4.46) than the latter (log K_{ow} 3.94). The presence of metals decreased the adsorption capacity with this effect becoming stronger as the metal concentration increased because of competitive adsorption. The decrease in adsorption capacity reached its highest point in the presence of Cu and its lowest when Cd was present for reasons explained earlier. From the Langmuir model parameter K_L, another parameter R_L can be calculated by using the formula $R_L = 1 / (1+C_mK_L)$ (where C_m is the maximum initial concentration of sorbate) to assess whether the adsorption process is favourable or not. The calculated R_L values for the two PAHs in the presence of all concentrations of heavy metals were in the range of 0.05 - 0.26. As these values are between 0 and 1, the adsorption process can be considered a favourable one [39].

Unlike PAHs adsorption, the adsorption of heavy metals alone or in the presence of PAHs did not fit to either of the two adsorption models. This is because the percentage removal of these metals was low at the low GAC doses used in the study and the intense competition of PAHs with heavy metals for adsorption.

Table 3. Model parameters for the adsorption of acenaphthylene on GAC at three metals concentrations in the presence of 0.005 M $NaNO_3$.

Metals		Langmuir model			Freundlich model			Dubinin–Radushkevick model			
		q_m	K_L	R^2	K_f	n	R^2	q_m	β	R^2	E
	mg/L	mg/g	L/mg		$mg/g(L/mg)^{1/n}$			mg/g	(mol^2/kJ^2)		(kJ/mol)
	0	2.63	6.40	0.75	2.63	2.69	0.58	3.2	0.04	0.88	3.5
Cu	5	0.81	7.87	0.73	1.79	3.59	0.39	1.4	0.05	0.65	3.13
Zn		0.88	9.32	0.75	2.35	2.11	0.58	2	0.03	0.40	3.9
Cd		1.98	9.29	0.73	1.87	4.35	0.33	4.4	0.14	0.36	1.9
Cu	20	0.54	4.84	0.74	1.19	3.17	0.20	1.21	0.04	0.53	3.4
Zn		0.57	5.44	0.64	1.09	4.10	0.18	1.9	0.09	0.73	2.4
Cd		1.87	13.08	0.88	1.59	9.93	0.12	1.7	0.08	0.20	2.4
Cu	50	0.31	2.88	0.67	2.79	0.76	0.48	2.94	0.05	0.78	3.3
Zn		0.51	3.55	0.60	1.91	11.38	0.26	1.9	0.01	0.51	6.3
Cd		0.96	10.66	0.62	1.15	2.28	0.17	2.7	0.09	0.46	2.3

Table 4. Model parameters for the adsorption of phenanthrene on GAC at three metals concentrations in the presence of 0.005 M $NaNO_3$.

Metals		Langmuir model			Freundlich model			Dubinin–Radushkevick model			
		q_m	K_L	R^2	K_f	n	R^2	q_m	β	R^2	E
	mg/L	mg/g	L/mg		mg/g(L/mg)$^{1/n}$			mg/g	(mol^2/kJ^2)		(kJ/mol)
	0	7.36	3.15	0.80	7.35	1.61	0.92	5.4	0.03	0.90	4
Cu	5	5.95	2.93	0.84	5.99	1.56	0.86	5.1	0.04	0.87	3.5
Zn		5.46	3.19	0.80	5.19	1.77	0.84	3.3	0.03	0.66	3.8
Cd		6.17	3.43	0.78	5.81	1.80	0.87	1.5	0.03	0.39	4
Cu	20	2.18	24.84	0.81	3.63	2.36	0.71	4.1	0.03	0.74	4.2
Zn		2.25	14.50	0.73	4.34	2.19	0.76	2.4	0.02	0.40	5.1
Cd		2.74	19.42	0.85	4.34	2.19	0.76	2.0	0.03	0.29	4.3
Cu	50	0.74	6.07	0.67	1.02	2.91	0.22	4.9	0.03	0.79	4.1
Zn		1.29	18.23	0.80	2.85	1.77	0.42	2.7	0.02	0.67	4.5
Cd		2.20	8.09	0.82	3.18	2.50	0.60	1.6	0.05	0.39	3.1

3.5. Kinetic adsorption modelling

The pseudo-first order model fitted better to the adsorption kinetic data of PAHs in the presence of heavy metals compared to the pseudo-second order model (Table S1). Conversely, the opposite trend occurred for the adsorption of heavy metals in the presence of PAHs (Table S2). This indicates that PAHs are adsorbed generally by physical interaction with GAC through hydrophobic interaction and van der Waals forces whereas heavy metals are adsorbed chemically through exchange with protons in the functional groups on GAC. These results are consistent with the zeta potential findings where heavy metals adsorption markedly decreased the negative charges on GAC and even Cu reversed them into positive charges (Figs. 6 and 7). In comparison, PAHs adsorption had only little effect on the zeta potential of GAC.

Because the GAC has numerous pores and channels, the kinetics of adsorption would have been influenced by PAHs' and metals' diffusion rates into these pores and channels. This was investigated by fitting the data to the Weber and Morris model [30]. The fit of the data showed two distinct sets of straight lines with high R^2 values (0.89-0.99) (Figs. 10 and 11, Table 5). The straight-line relationships' and the initial line going through the origin in the graph show that the rate of adsorption is controlled by intra-particle diffusion. The straight-line plots indicate that initially the rate of adsorption was fast (high K_{s1}) followed by a slower rate of adsorption (low K_{s2}) (Table 5). The faster rate of adsorption was probably due to intra-particle diffusion into the mesopores and the slower rate was into the micropores. Haro et al. [40] reported three straight lines when the data for the adsorption of acenaphthene and fluorene on activated carbon were plotted according to Weber and Morris model. They attributed the first line up to 10 min to external mass transfer and the other two from 10 min to 4 h to intra-particle diffusion similar to our interpretation. The allocation of the data to the two straight lines is arbitrary by eye-estimate using the limited data which is clear for PAHs but not so much for the metals. Therefore, more data are required especially at longer times in future studies to confirm the above explanations.

The diffusion rate into the mesopores (K_{s1}) was faster for acynaphthylene (molar volume 168 cm^3/mol) than that for phenanthrene (molar volume 199 cm^3/mol) irrespective of the type of metals present because of its smaller size. However, this pattern was not noticed in the rate of diffusion into the micropores (K_{s2}). With reference to the metals, generally, no difference in the rate of diffusion into the mesopores was observed, but in the micropores the heavy metals' rate of diffusion was higher than that of PAHs.

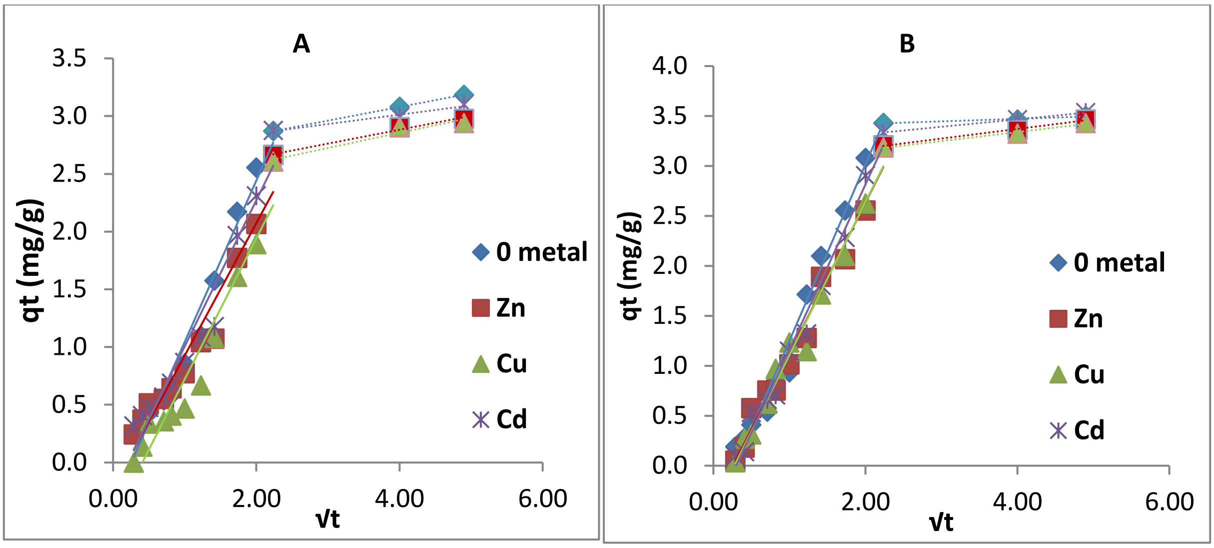

Fig. 10. Weber and Morris plots of (A) rate of adsorption of phenanthrene in the presence of heavy metals; (B) rate of adsorption of acynaphthylene in the presence of heavy metals (PAH 1 mg/L, metals 20 mg/L, GAC dose 0.3 g/L).

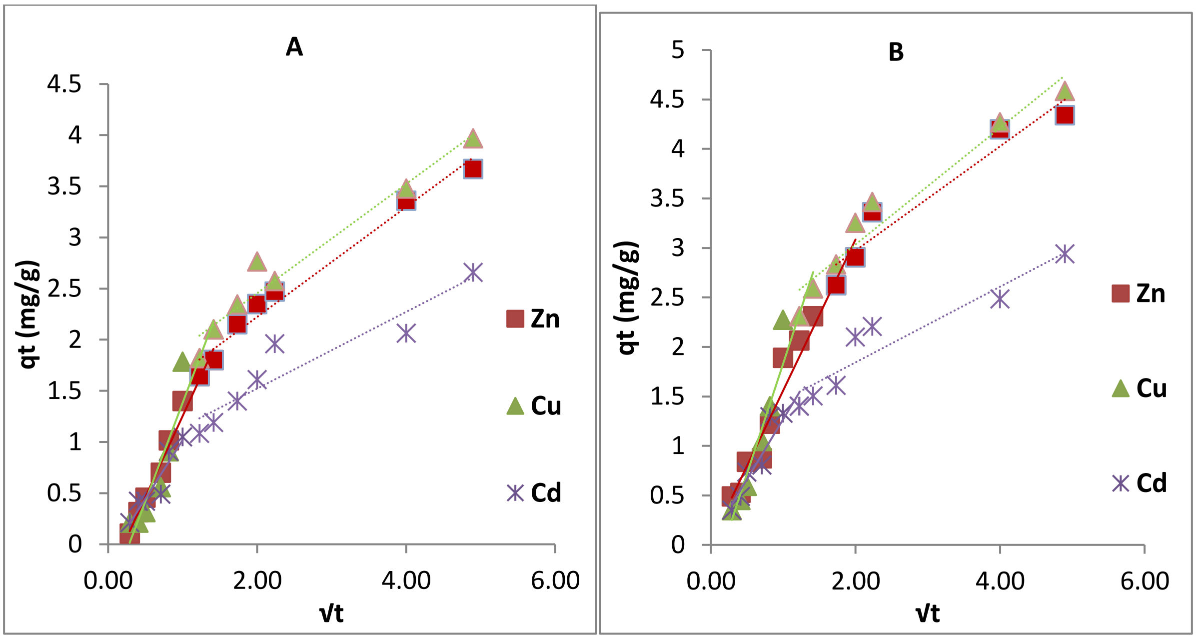

Fig. 11. Weber and Morris plots of (A) rate of adsorption of metals in the presence of phenanthrene; (B) rate of adsorption of metals in the presence of acynaphthylene (1 mg/L) (PAH 1 mg/L, metals 20 mg/L, GAC dose 0.3 g/L).

Table 5. Weber-Morris plot parameters for the adsorption of PAHs and heavy metals in the presence of each other

		Weber-Morris short-term adsorption		Weber-Morris long-term adsorption	
PAH	Metal	K_{s1} mg/g /min$^{1/2}$	R^2	K_{s2} mg/g /min$^{1/2}$	R^2
Acenaphthylene	0	1.76	0.985	0.025	0.966
	Cd	1.66	0.987	0.075	0.999
	Zn	1.51	0.979	0.096	0.995
	Cu	1.52	0.982	0.09	0.989
Phenanthrene	0	1.39	0.968	0.12	1.000
	Cd	1.26	0.949	0.08	0.969
	Zn	1.15	0.947	0.12	0.984
	Cu	1.19	0.926	0.13	0.942
Metals with acenaphthylene	Cd	1.14	0.894	0.38	0.887
	Zn	1.47	0.980	0.51	0.979
	Cu	1.92	0.932	0.53	0.957
Metals with phenanthrene	Cd	1.24	0.913	0.27	0.987
	Zn	1.16	0.977	0.40	0.969
	Cu	1.28	0.960	0.43	0.935

4. Conclusions

In solutions containing both PAHs (acenaphthylene or phenanthrene) and heavy metals (Cd, Cu or Zn) the adsorptive removal of PAHs using GAC was greater than those of heavy metals, even with the latter at 20 times higher concentration. The adsorptive capacities of both PAHs and heavy metals were reduced in the presence of both compared to their capacities when they were present separately. This was due to competition for adsorption, despite their adsorption mechanisms being different. Copper and Zn reduced the adsorption of PAHs more than Cd did. Similarly, PAHs reduced the adsorption of Cd more than the other metals. These results were explained using zeta potential data where Cu and Zn reduced the negative charges on the GAC more than Cd did – the negative charges were even reversed to positive values in the presence of Cu. The adsorption capacity was higher for phenanthrene than for acenaphthylene, which was consistent with the higher hydrophobicity of phenanthrene. The Langmuir adsorption capacity for both the PAHs decreased with increased concentration of metals, the effect being in the order Cu > Zn > Cd. The kinetic adsorption data fitted to the Weber and Morris plots indicating intra-particle diffusion of both PAHs and heavy metals into the mesopores and micropores in GAC. The diffusion rate was higher in all cases in the mesopores which occurred when the adsorption process began. The rate of diffusion into mesopores was faster for acenaphthylene than phenanthrene irrespective of the type of metal present, consistent with their size difference. The rate of diffusion in both mesopores and micropores was in the order Cu > Zn > Cd in the presence of either of the PAHs.

Acknowledgement

This study was financially supported by the Cooperative Research Centre for Contamination Assessment and Remediation of the Environment (CRC CARE) (project number 4.1.15.12/13).

References

[1] M. Ahmaruzzaman, Industrial wastes as low-cost potential adsorbents for the treatment of wastewater laden with heavy metals, Adv. Colloid Interface Sci. 166 (2011) 36-59.

[2] H.I. Abdel-Shafy, M.S.M. Mansour, A review on polycyclic aromatic hydrocarbons: Source, environmental impact, effect on human health and remediation, Egyptian J. Petroleum 25 (2016) 107-123.

[3] B. Armstrong, E. Hutchinson, J. Unwin, T. Fletcher, Lung cancer risk after exposure to polycyclic aromatic hydrocarbons: a review and meta-analysis, Environ. Health Perspect. 112 (2004) 970-978.

[4] F. Fu, Q Wang, Removal of heavy metal ions from wastewater: A review, J. Environ. Manage. 92 (2011) 407-418.

[5] A.K. Haritash, C.P. Kaushik, Biodegradation aspects of polycyclic aromatic hydrocarbons (PAHs): a review, J. Hazard. Mater. 169 (2009) 1-15.

[6] A.T. Lawal, Polycyclic aromatic hydrocarbons: A review, Cogent Environ. Sci. 3 (2017) 1339841, 89 pages.

[7] P.T. Gauthier, W.P. Norwood, E.E. Prepas, G.G. Pyle, Metal-PAH mixtures in the aquatic environment: a review of co-toxic mechanisms leading to more-than-additive outcomes, Aquat. Toxicol. 154 (2014) 253–269.

[8] S.E. Baily, T.J. Olin, R.M. Bricka, D.D. Adrian, A review of potentially low-cost sorbents for heavy metals, Water Res. 33 (199) 2469-2479.

[9] M. Hua, S. Zhang, B. Pan, W. Zhang, L. Lv, Q. Zhang, Heavy metal removal from water/wastewater by nanosize metal oxides: A review, J. Hazard. Mater. 211-212 (2012) 317-331.

[10] S. Lamichhane, K.C. Balkrishna, R. Sarukkalige, Polycyclic aromatic hydrocarbons (PAHs) removal by sorption: A review, Chemosphere 148 (2016) 336-353.

[11] S.M. Yakout, A.A. Daifullah, S.A. El-Reefy, Adsorption of naphthalene, phenanthrene and pyrene from aqueous solution using low-cost activated carbon derived from agricultural wastes, Adsorpt. Sci. Technol. 31 (2013) 293-302.

[12] D. Eeshwarasinghe, P. Loganathan, M. Kalaruban, D.P. Sounthararajah, J. Kandasamy, S. Vigneswaran, Removing polycyclic aromatic hydrocarbons from water using granular activated carbon: kinetic and equilibrium adsorption studies, Environ. Sci. Pollut. Res. 25 (2018) 13511-13524.

[13] C. Valderrama, X. Gamisans, J.L. Cortina, A. Farrán, F.X. De las Heras, Evaluation of polyaromatic hydrocarbon removal from aqueous solutions using activated carbon and hyper-crosslinked polymer (Macronet MN200), J. Chem. Technol. Biotechnol. 84 (2009) 236-245.

[14] Y. Tao, W. Li, B. Xue, J. Zhong, S. Yao, Q. Wu, Different effects of copper (II), cadmium (II), and phosphate on the sorption of phenanthrene on the biomass of cyanobacteria, J. Hazard. Mater. 261 (2013) 21-28.

[15] P. Loganathan, S. Vigneswaran, J. Kandasamy, Road-deposited sediments pollutants: a critical review of their characteristics, source apportionment, and management, Crit. Rev. Environ. Sci. Technol.43 (2013) 1315-1348.

[16] T.C. Nguyen, Pollutants in road-deposited sediments: characteristics, mobility, bioavailability and remediation. Ph D thesis submitted to University of Technology Sydney, Australia (2006).

[17] J. Chen, D. Zhu, C. Sun, Effect of heavy metals on the sorption of hydrophobic organic compounds to wood charcoal, Environ. Sci. Technol. 41 (2007) 2536-2541.

[18] Y. Huang, A.N. Fulton, A.A. Keller, Simultaneous removal of PAHs and metal contaminants from water using magnetic nanoparticle adsorbents, Sci. Total Environ. 571 (2016) 1029-1036.

[19] J. Aissaoui, M. Kacem, P. Dubujet, A. Mgaidi, Study of multi compound sorption of lead and pyrene on a reconstituted soil: batch and fixed bed column tests, Soil Sediment Contam. 26 (20170 404-425.

[20] Z. Zhang, X. Hou, X. Zhang, H. Li, The synergistic adsorption of pyrene and copper onto Fe(III)functionalized mesoporous silica from aqueous solution, Colloids and Surfaces A: Physicochem. Eng. Aspects 520 (2017) 39-45.

[21] M. Saeedi, L.Y. Li, J.R. Grace, Effect of organic matter and selected heavy metals on sorption of acenaphthene, fluorene and fluoranthene onto various clays and clay minerals. Environ. Earth Sci. 77 (2018) 305.

[22] Y. Tao, B. Xue, Z. Yang, S. Yao, S. Li, Effects of heavy metals on the sorption of polycyclic aromatic hydrocarbons by *Microcystis aeruginosa*. J. Environ. Qual. 43 (2014) 1953-1962.

[23] T.A. Kurniawan, G.Y.S. Chan, W. Lo, S. Babel, Comparisons of low-cost adsorbents for treating wastewaters laden with heavy metals, Sci. Total Environ. 366 (2006) 409-426.

[24] P. Loganathan, W.G. Shim, D.P. Sounthararajah, M. Kalaruban, T. Nur, S. Vigneswaran, Modelling equilibrium adsorption of single, binary, and ternary combinations of Cu, Pb, and Zn onto granular activated carbon, Environ. Sci. Pollut. Res. 25 (2018) 16664-16675.

[25] D.P. Sounthararajah, P. Loganathan, J. Kandasamy, S. Vigneswaran, Column studies on the removal of dissolved organic carbon, turbidity and heavy metals from stormwater using granular activated carbon, Desalin. water Treat. 57 (2016) 5045-5055.

[26] A.O. Alade, O.S. Amuda, A.O. Ibrahim, Isothermal studies of adsorption of acenaphthene from aqueous solution onto activated carbon produced from rice (Oryza sativa) husk, Environ. Sci. Technol. 46 (2012) 87-95.

[27] L.J. Westholm, E. Repo, M. Sillanpaa, Filter materials for metal removal from mine drainage – a review, Environ. Sci. Pollut. Res. 21 (2014) 9109-9128.

[28] M. Manjuladevi, O.M. Sri, Heavy metals removal from industrial wastewater by nano adsorbent prepared from cucumis melopeel activated carbon, J. Nanomed. Res. 5 (2017) 00102, 4 pages.

[29] M. Kalaruban, P. Loganathan, W.G. Shim, J. Kandasamy, H.H. Ngo, S. Vigneswaran, Enhanced removal of nitrate from water using amine-grafted agricultural wastes, Sci. Total Environ. 565 (2016) 503-510.

[30] W.J. Weber, J.C. Morris, Kinetics of adsorption on carbon from solution, J. Sanit. Eng. Div. - ASCE 89 (1963) 31-59.

[31] L. Dong, L. Hou, Z. Wang, P. Gu, G. Chen, R. Jiang, A new function of spent activated carbon in BAC process: Removing heavy metals by ion exchange mechanism, J. Hazard. Mater. 359 (2018) 76-84.

[32] X. Ge, Z. Wu, Z. Wu, Y. Yan, G. Cravotto, B. Ye, Enhanced PAHs adsorption using iron-modified coal-based activated carbon via microwave radiation, J. Taiwan Inst. Chem. Eng. 64 (2016) 235-243.

[33] D.P. Sounthararajah, P. Loganathan, J. Kandasamy, S. Vigneswaran, Effects of humic acid and suspended solids on the removal of heavy metals from water by adsorption onto granular activated carbon, Inter. J. Environ. Res. Public Health 12 (2015) 10475-10489.

[34] A. Erto, F. Di Natale, D. Musmarra, A.Lancia, Modeling of single and competitive adsorption of cadmium and zinc onto activated carbon, Adsorption 21 (2015) 611-621.

[35] M.B. McBride, Reactions controlling heavy metal solubility in soil, Adv. Soil Sci. 10 (1989) 1–56.

[36] K. Park, C. Lee, S. Ryu, X. Yang, Zeta-potentials of oxygen and nitrogen enriched activated carbons, Carbon Letters 8 (2007) 321-325.

[37] S.A. Dastgheib, D.A. Rockstraw, Pecan shell activated carbon: synthesis, characterization, and application for the removal of copper from aqueous solution, Carbon 39 92001) 1849-1855.

[38] T.M. Little, F.J. Hills, Agricultural Experimentation, Design and Analysis, John Willey and Sons, New York. (1978).

[39] R. Rusmin, B. Sarkar, Y. Liu, S. McClure, R. Naidu, Structural evolution of chitosan–palygorskite composites and removal of aqueous lead by composite beads, Appl. Surf. Sci. 353 (2015) 363-375.

[40] M. Haro, B. Cabal, J.B. Parra, C.O. Ania, On the adsorption kinetics and equilibrium of polyaromatic hydrocarbons from aqueous solution, Adsorp. Sci. Tech. 29 (2011) 467-478.

Supplementary Data

Simultaneous removal of polycyclic aromatic hydrocarbons and heavy metals from water using granular activated carbon

Dinushika Eeshwarasinghe, Paripurnanda Loganathan, Saravanamuthu Vigneswaran*

Faculty of Engineering, University of Technology Sydney (UTS), P.O. Box 123, Broadway, NSW 2007, Australia

Table S1. Kinetic model parameter values for the adsorption of acenaphthylene and phenanthrene on GAC in the presence of 0.005 M $NaNO_3$ (GAC 0.3 g/L, PAH 1 mg/L, Metals 20 mg/L).

PAH	Metal	Pseudo-first order			Pseudo-second order			Experimental
		q_m mg/g	k_1 h^{-1}	R^2	q_m mg/g	k_2 g/mg/h	R^2	q_m (mg/g)
Acenaphthylene	0	3.70	0.56	0.973	5.89	3.7	0.973	3.43
	Cu	3.25	0.37	0.974	4.00	0.34	0.809	3.18
	Zn	3.85	0.56	0.846	5.9	0.26	0.812	3.20
	Cd	4.30	0.66	0.872	6.93	0.18	0.642	3.34
Phenanthrene	0	3.05	0.56	0.948	3.66	0.42	0.686	2.87
	Cu	2.68	0.32	0.967	3.35	0.16	0.459	2.61
	Zn	2.34	0.25	0.825	3.57	0.43	0.794	2.66
	Cd	3.89	0.72	0.755	3.57	0.43	0.732	2.80

Table S2. Kinetic model parameter values for the adsorption of metals on GAC in the presence of acenaphthylene, phenanthrene and 0.005 M $NaNO_3$ (GAC 0.3 g/L, PAH 1 mg/L, Metals 20 mg/L)

Metal		Pseudo-first order			Pseudo-second order			Experimental
		q_m mg/g	k_1 h^{-1}	R^2	q_m mg/g	k_2 g/mg/h	R^2	q_m (mg/g)
Cu	0	3.94	0.29	0.919	4.64	0.66	0.996	4.67
Zn	0	3.7	0.26	0.969	4.54	0.61	0.989	4.34
Cd	0	2.31	0.24	0.894	2.42	1.17	0.961	2.94
Cu	Acenaphthylene	2.41	0.38	0.615	4.72	0.36	0.858	4.09
Zn	Acenaphthylene	2.22	0.38	0.615	4.29	0.42	0.914	3.95
Cd	Acenaphthylene	1.91	0.47	0.893	2.21	0.79	0.939	2.66
Cu	Phenanthrene	2.00	0.25	0.727	2.69	0.63	0.944	3.08
Zn	Phenanthrene	2.04	0.32	0.645	3.29	0.53	0.91	3.45
Cd	Phenanthrene	1.68	0.18	0.799	1.62	0.84	0.958	1.96

Fig. S1. Absorbance spectra for different concentrations of acenaphthylene and phenanthrene

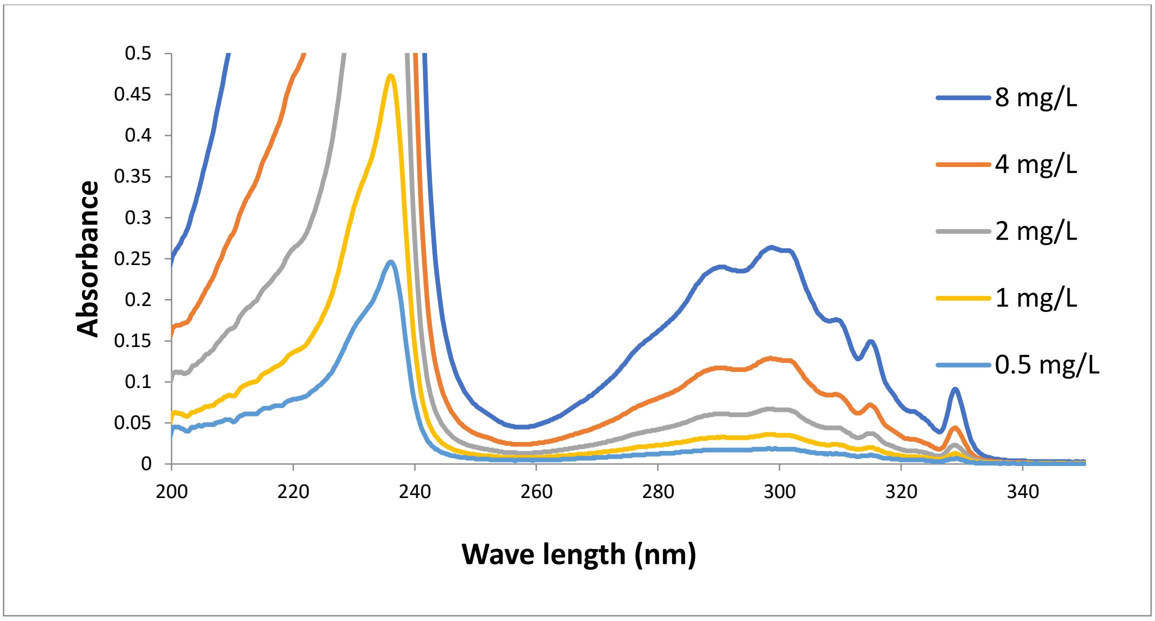

Acenaphthylene

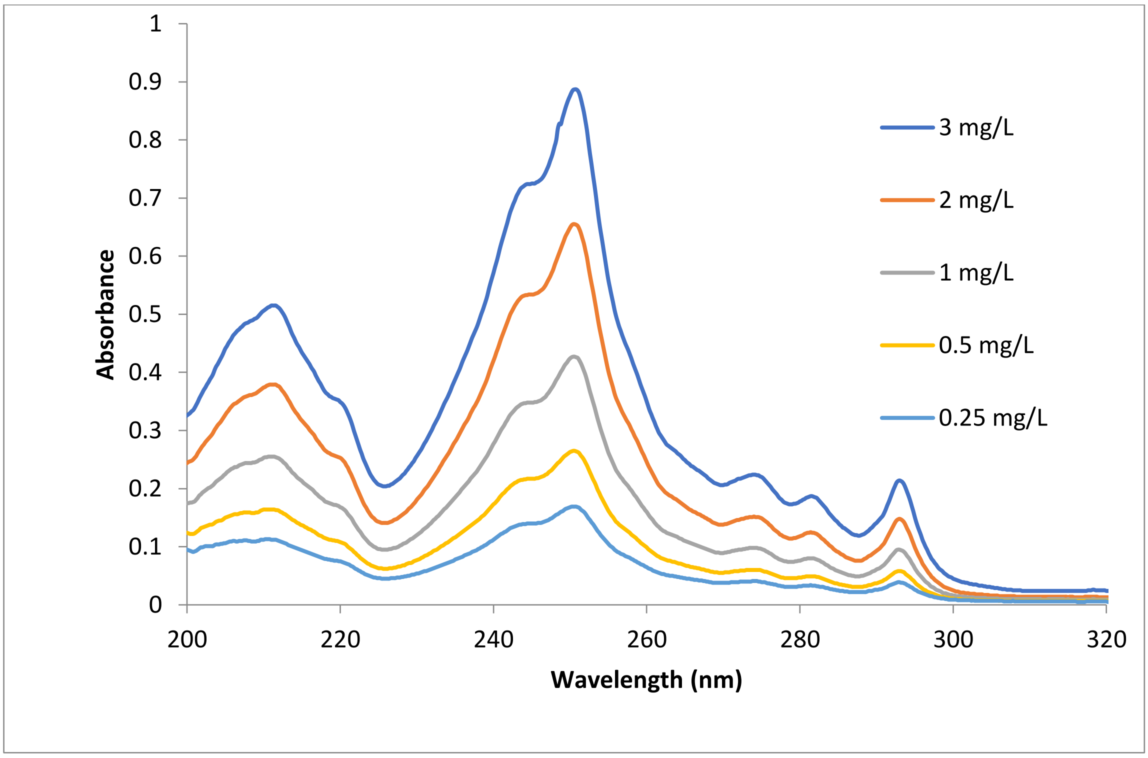

Phenanthrene

Fig. S2. Calibration graphs of absorbance vs PAH concentration

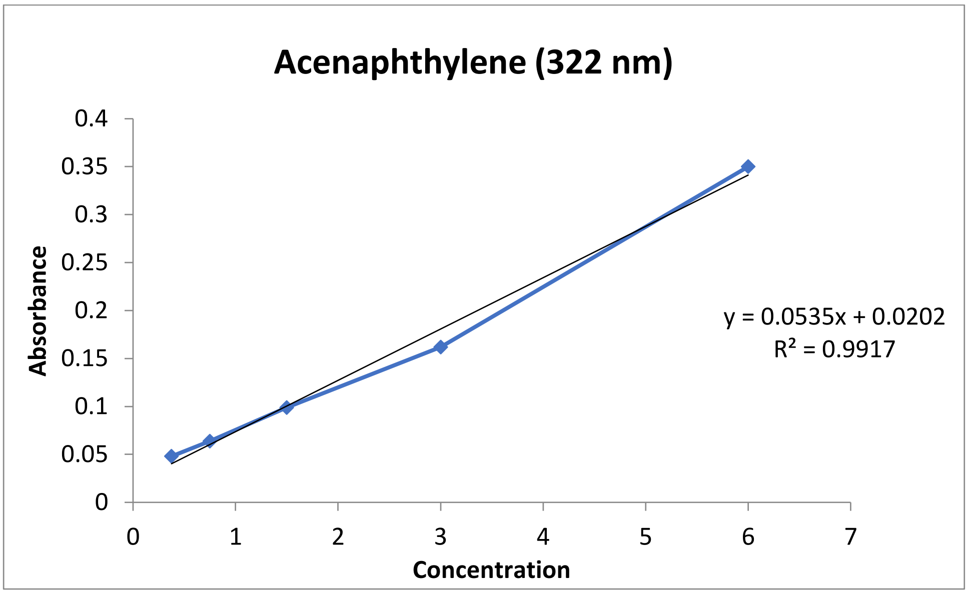

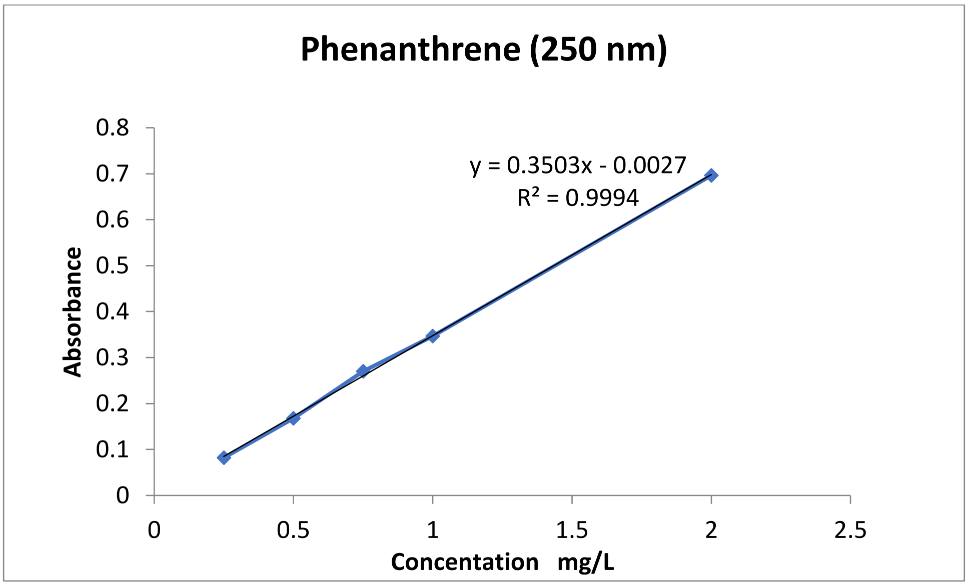

Fig. S3. Absorbance spectra for acenaphthylene (1 mg/L) in the presence of different concentrations of Cu, Zn, and Cd

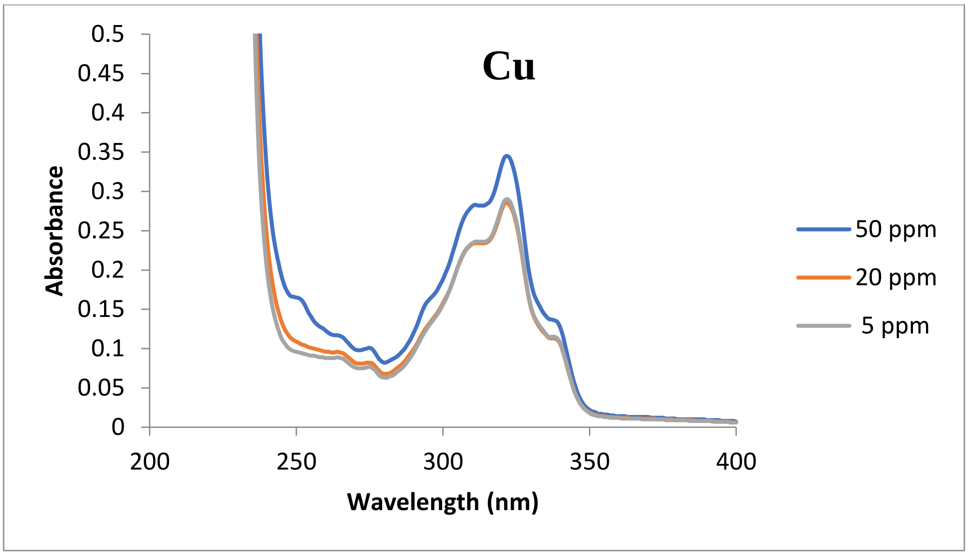

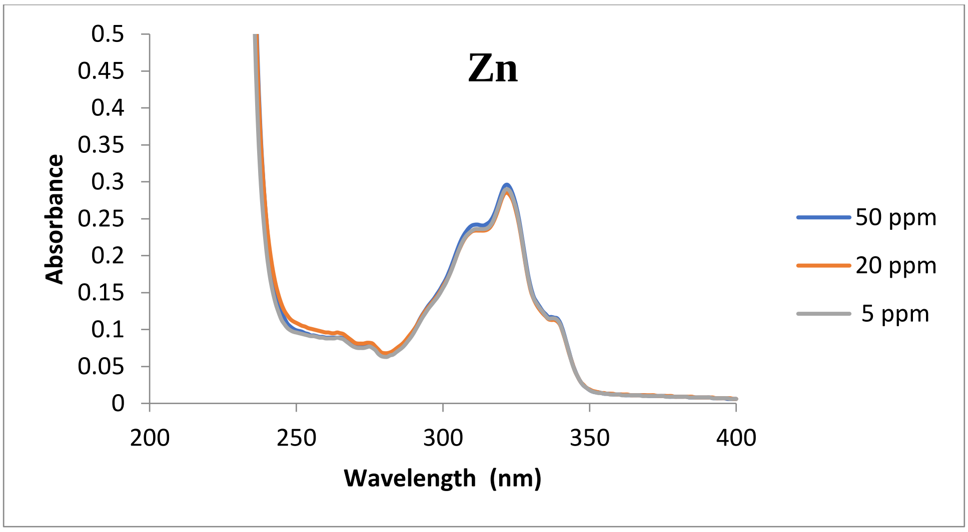

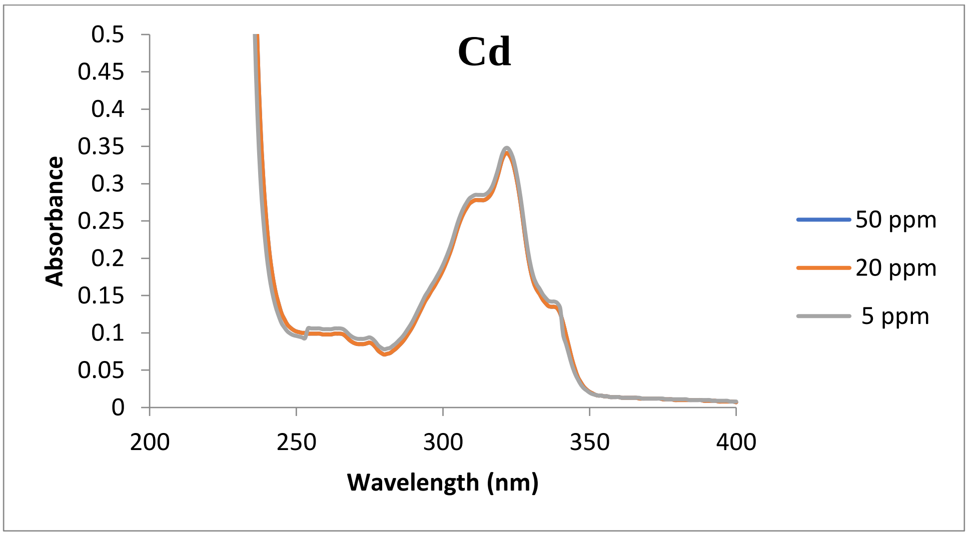

Fig. S4. Absorbance spectra for phenanthrene (1 mg/L) in the presence of different concentrations of Cu, Zn, and Cd

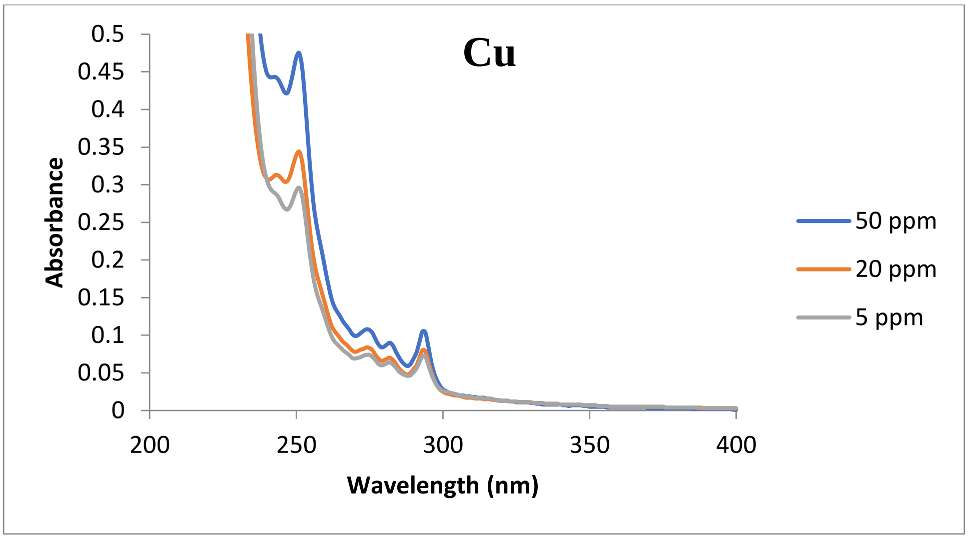

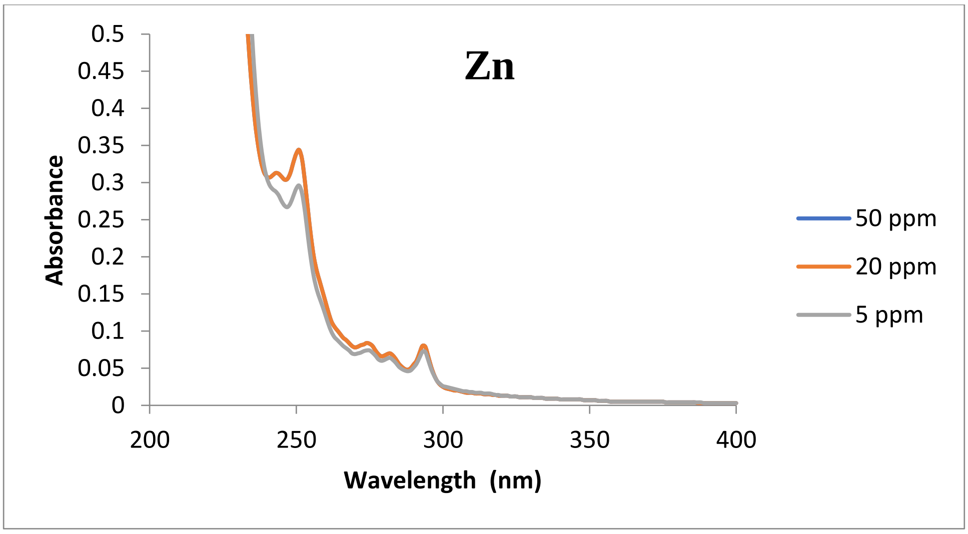

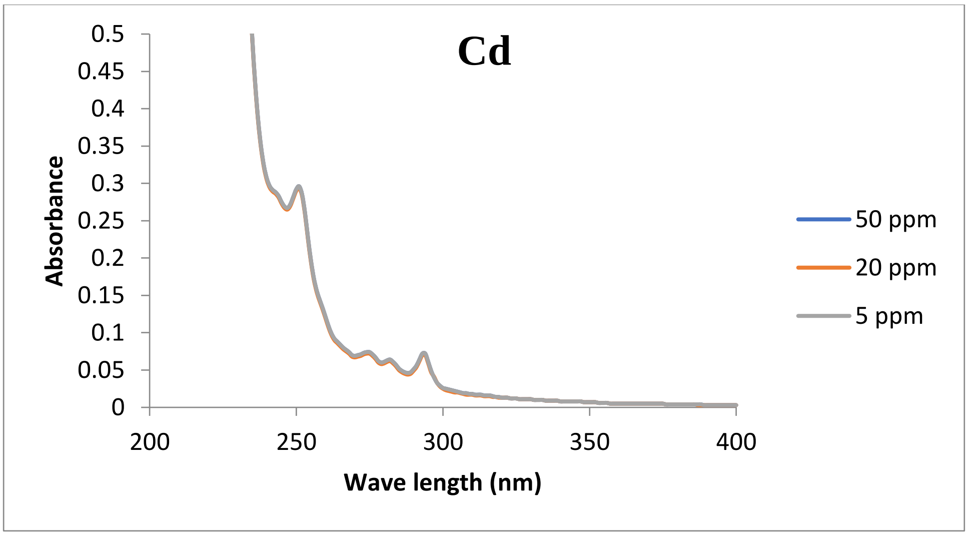

Fig. S5. Absorbance spectra of different concentrations of acenaphthylene in the presence of 50 mg/L of metals

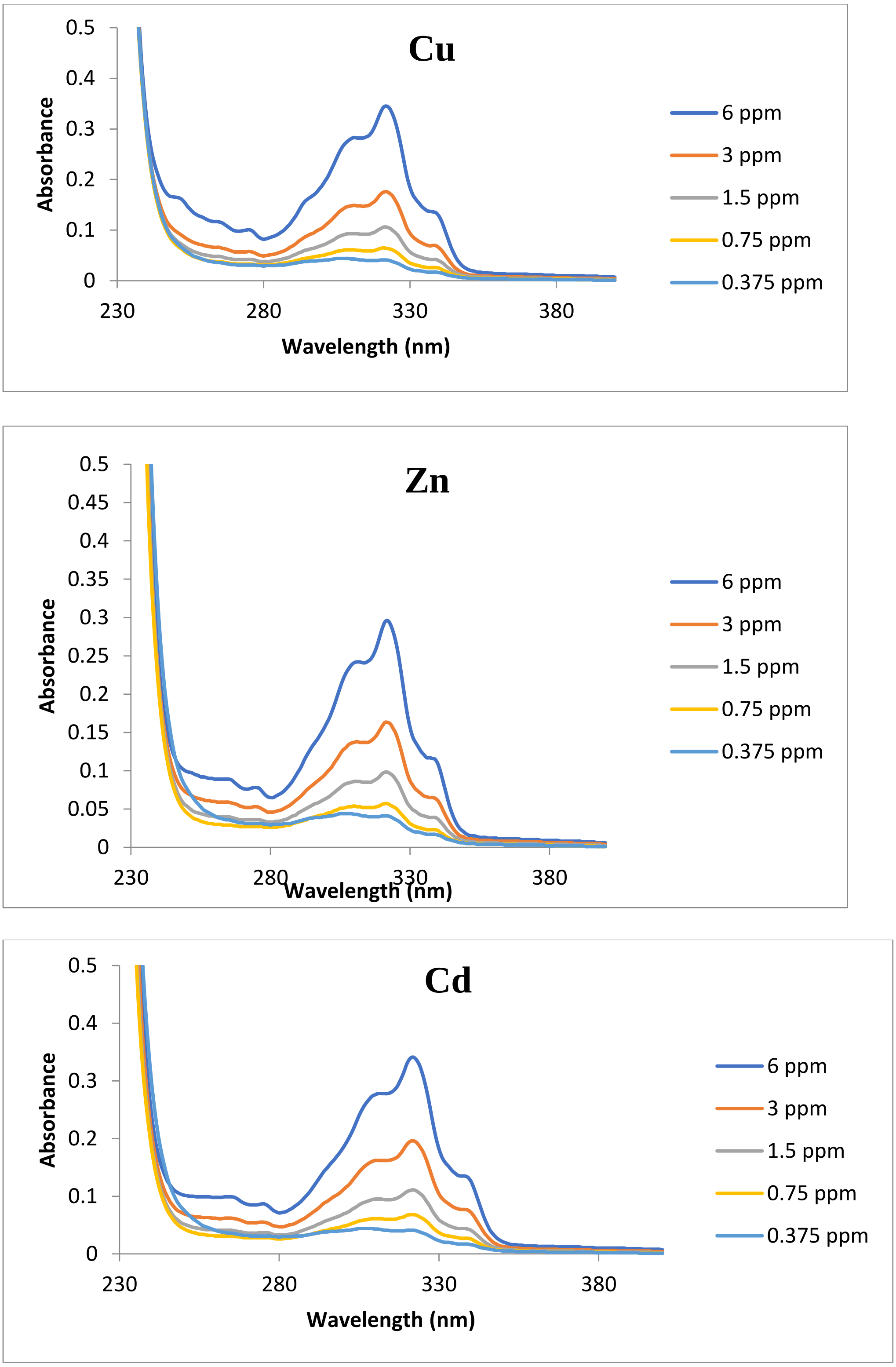

Fig. S6. Absorbance spectra of different concentrations of phenanthrene in the presence of 50 mg/L of metals

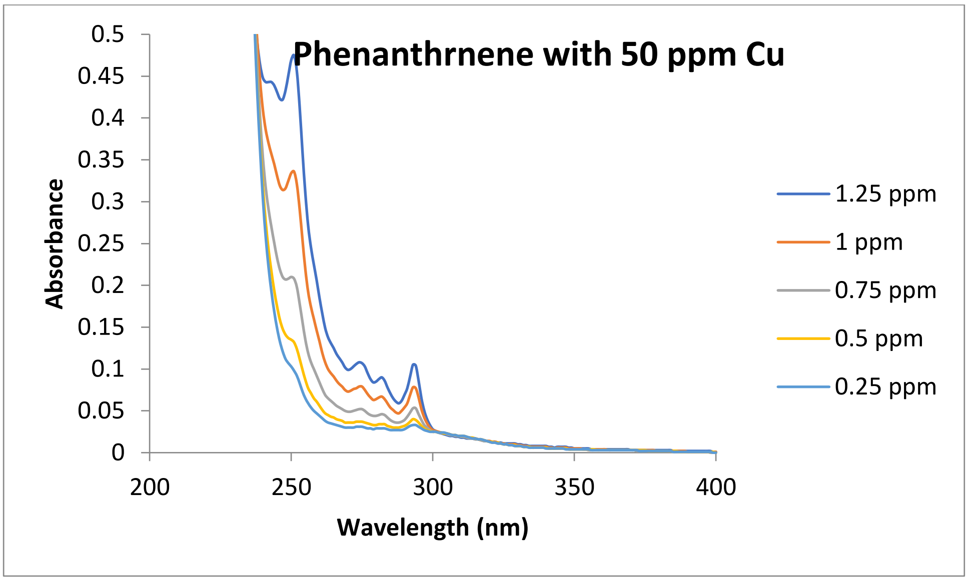

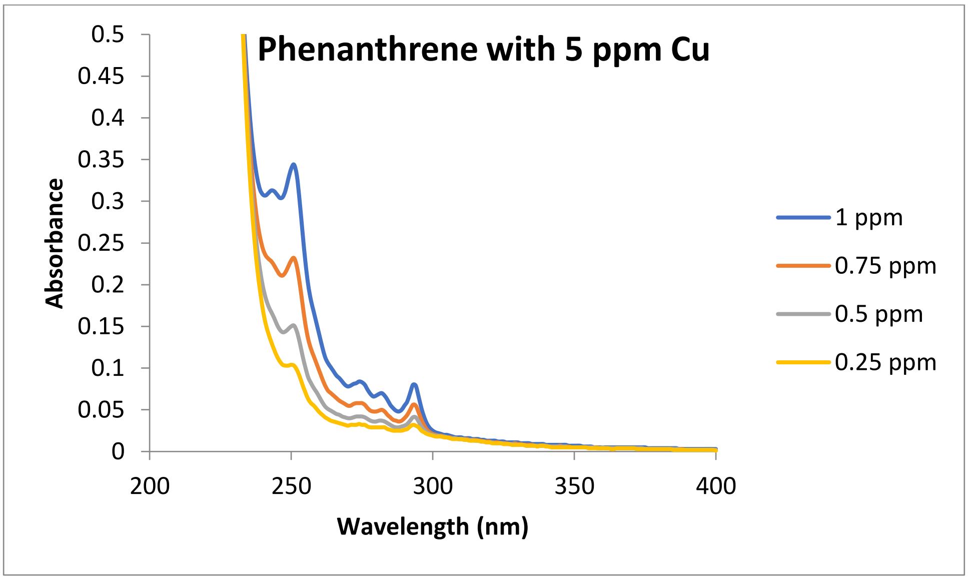

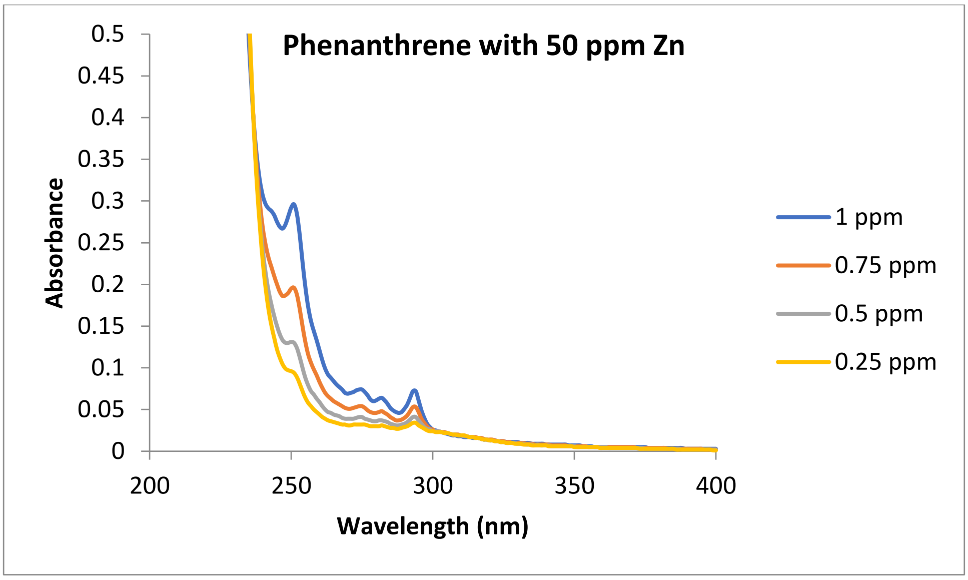
Phenanthrene with 50 ppm Zn
Absorbance
0.5
0.45
0.4
0.35
0.3
0.25
0.2
0.15
0.1
0.05
0
200
250
300
350
400
Wavelength (nm)
1 ppm
0.75 ppm
0.5 ppm
0.25 ppm

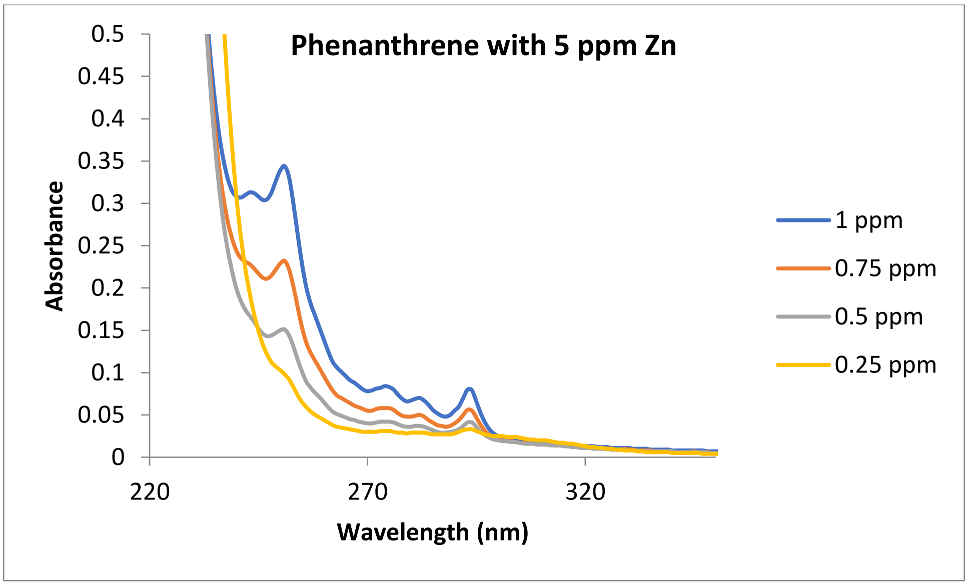
Phenanthrene with 5 ppm Zn
Absorbance
0.5
0.45
0.4
0.35
0.3
0.25
0.2
0.15
0.1
0.05
0
220
270
320
Wavelength (nm)
1 ppm
0.75 ppm
0.5 ppm
0.25 ppm

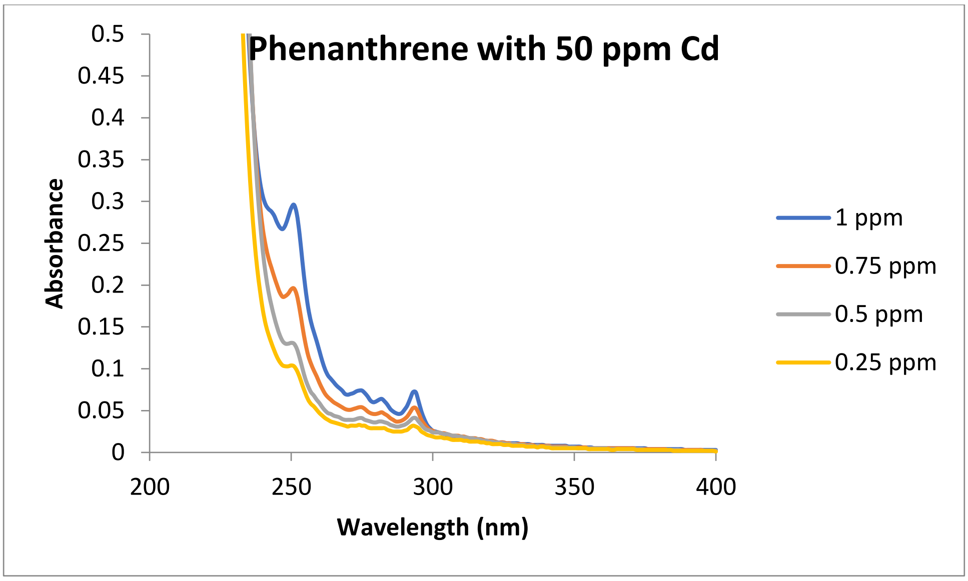
Phenanthrene with 50 ppm Cd
Absorbance
0.5
0.45
0.4
0.35
0.3
0.25
0.2
0.15
0.1
0.05
0
200
250
300
350
400
Wavelength (nm)
1 ppm
0.75 ppm
0.5 ppm
0.25 ppm

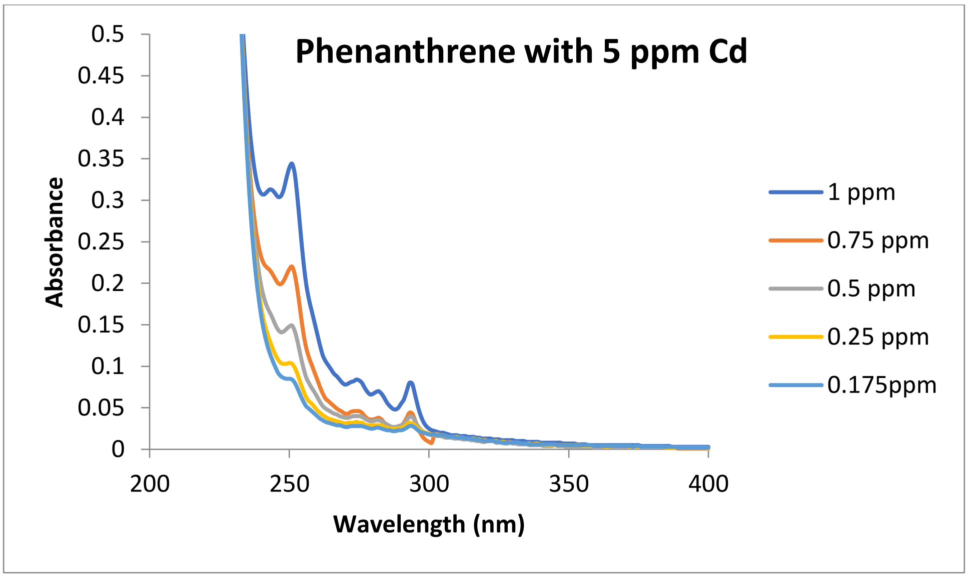
Phenanthrene with 5 ppm Cd
Absorbance
0.5
0.45
0.4
0.35
0.3
0.25
0.2
0.15
0.1
0.05
0
200
250
300
350
400
Wavelength (nm)
1 ppm
0.75 ppm
0.5 ppm
0.25 ppm
0.175ppm

Fig. S7: Standard calibration curves for acenaphthylene

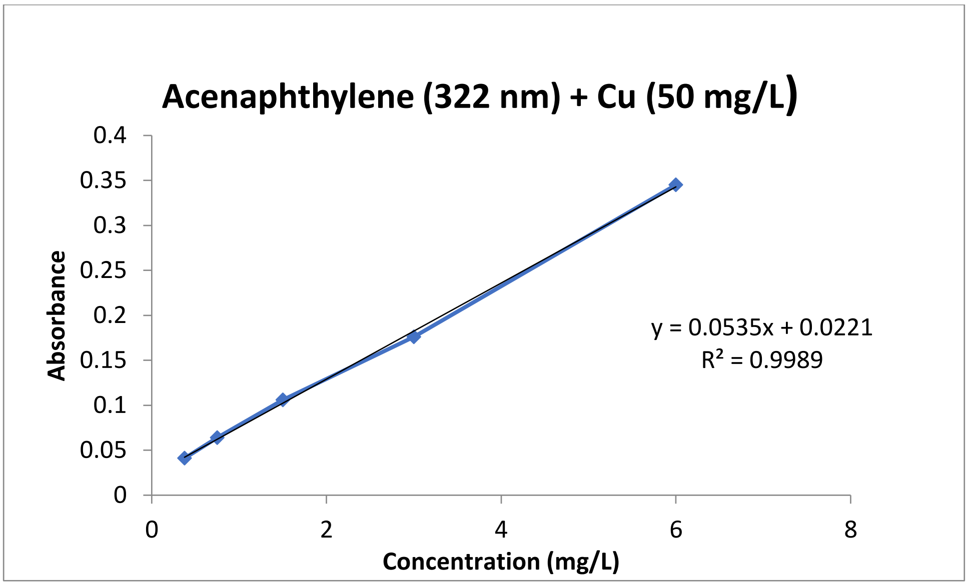

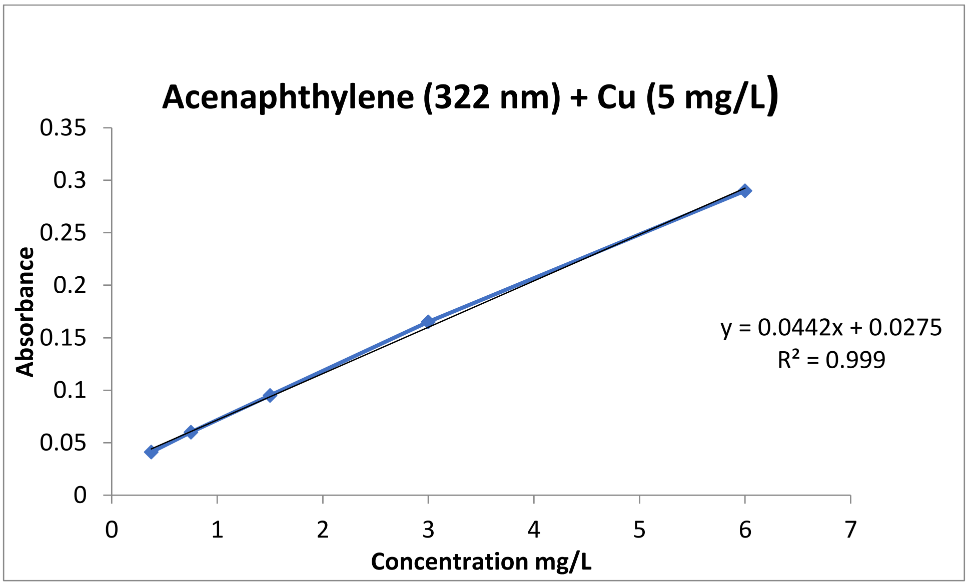

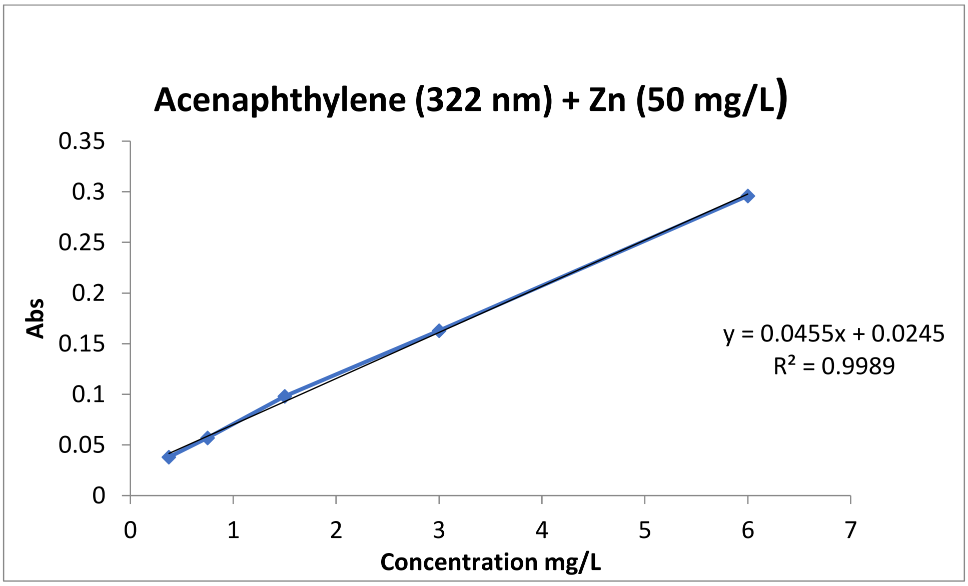

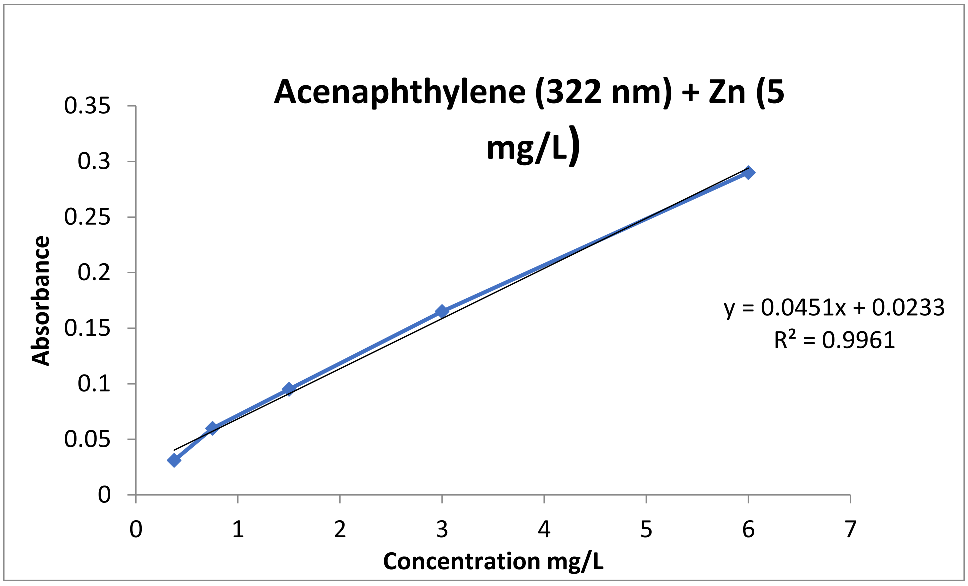
Acenaphthylene (322 nm) + Zn (5 mg/L)
Absorbance
0.35
0.3
0.25
0.2
0.15
0.1
0.05
0
0
1
2
3
4
5
6
7
Concentration mg/L
y = 0.0451x + 0.0233
R² = 0.9961

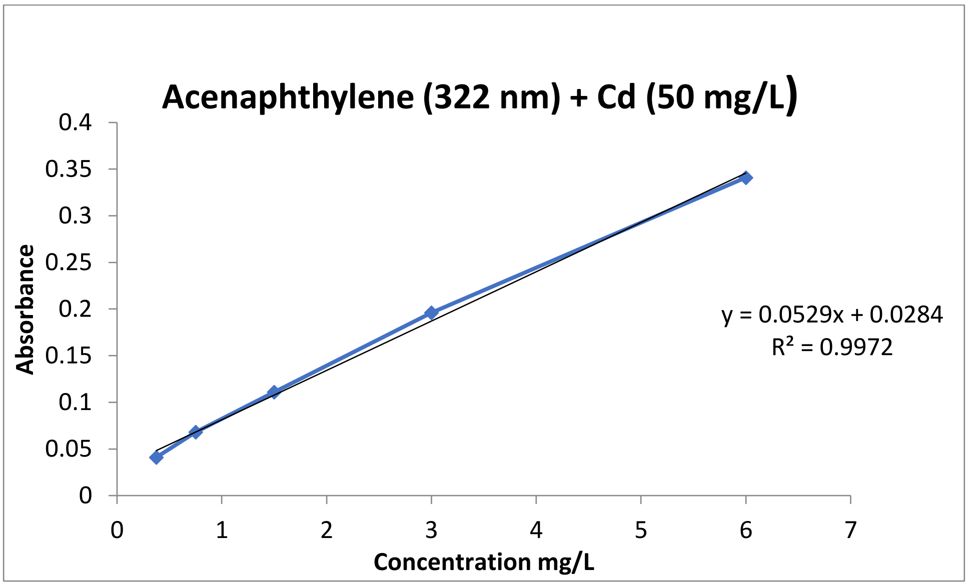
Acenaphthylene (322 nm) + Cd (50 mg/L)
Absorbance
0.4
0.35
0.3
0.25
0.2
0.15
0.1
0.05
0
0
1
2
3
4
5
6
7
Concentration mg/L
y = 0.0529x + 0.0284
R² = 0.9972

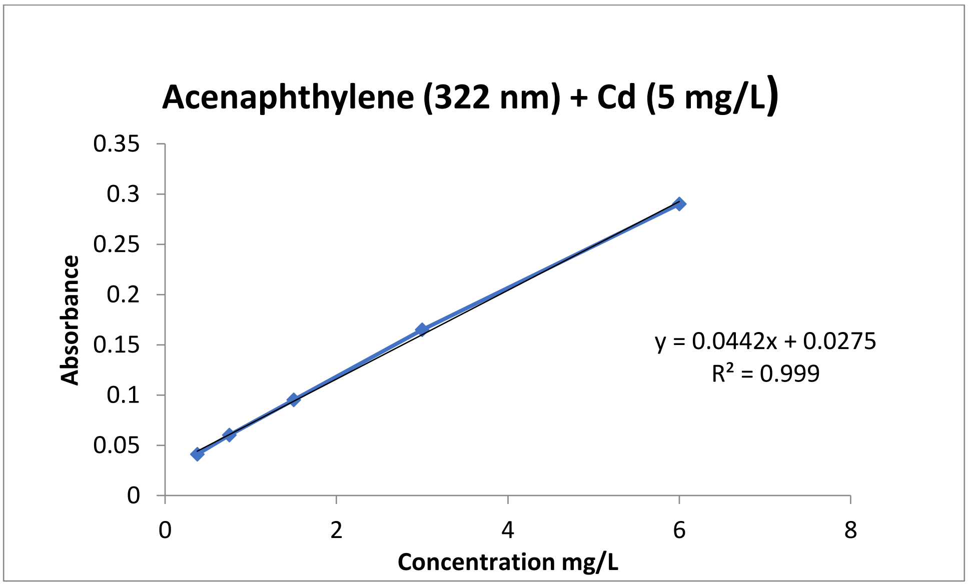
Acenaphthylene (322 nm) + Cd (5 mg/L)
Absorbance
0.35
0.3
0.25
0.2
0.15
0.1
0.05
0
0
2
4
6
8
Concentration mg/L
y = 0.0442x + 0.0275
R² = 0.999

Fig. S8: Standard calibration curves for phenanthrene

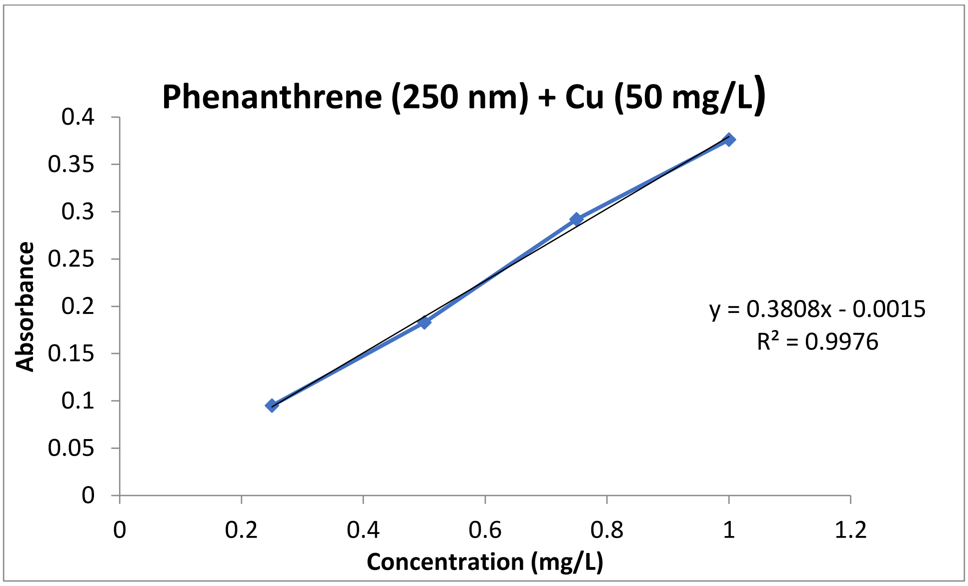

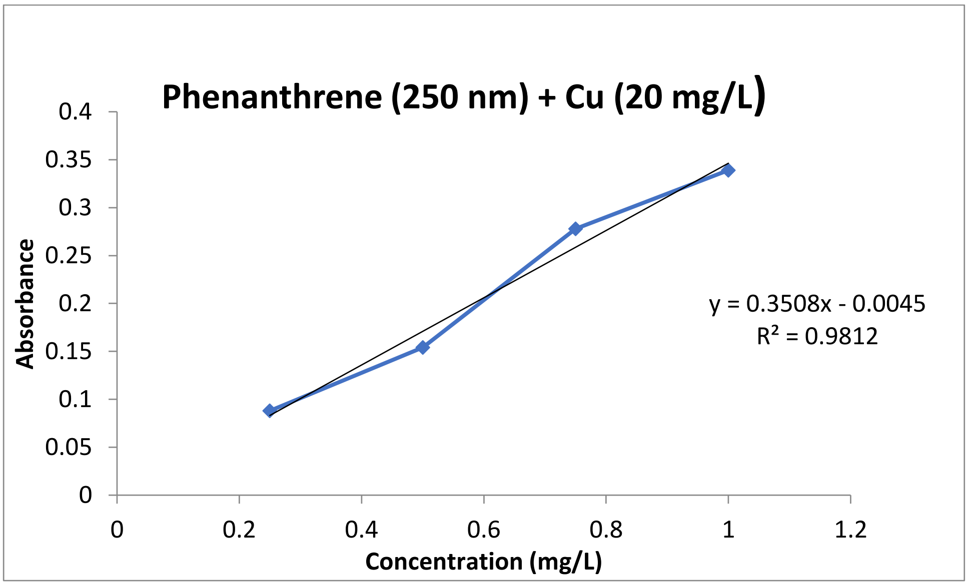

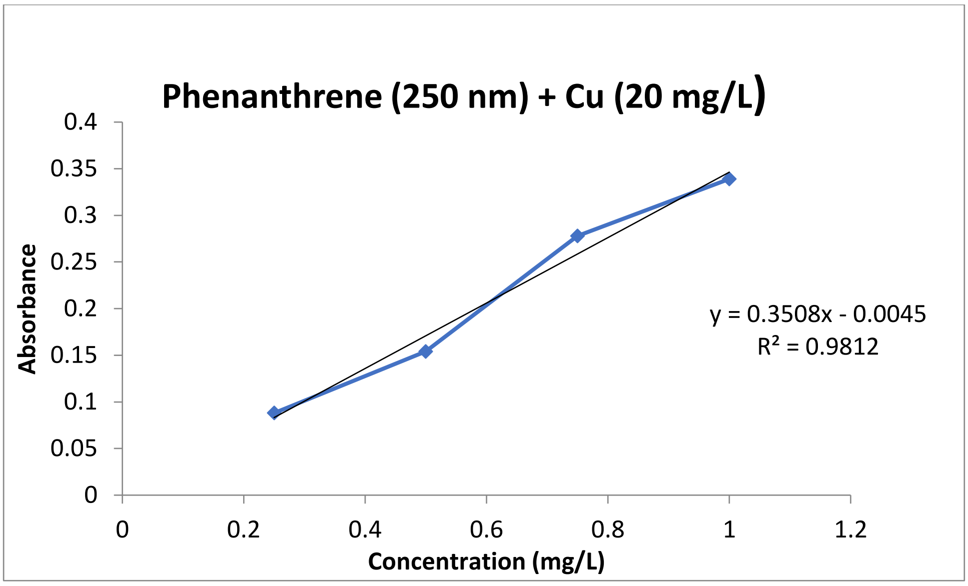
Phenanthrene (250 nm) + Cu (20 mg/L)
Absorbance
Concentration (mg/L)
0.4
0.35
0.3
0.25
0.2
0.15
0.1
0.05
0
0
0.2
0.4
0.6
0.8
1
1.2
y = 0.3508x - 0.0045
R² = 0.9812

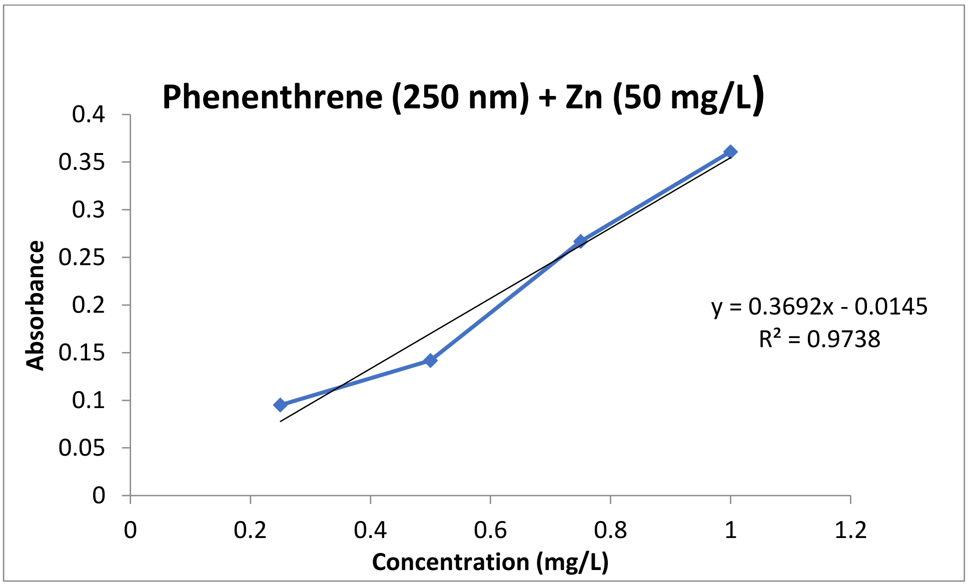
Phenenthrene (250 nm) + Zn (50 mg/L)
Absorbance
Concentration (mg/L)
0.4
0.35
0.3
0.25
0.2
0.15
0.1
0.05
0
0
0.2
0.4
0.6
0.8
1
1.2
y = 0.3692x - 0.0145
R² = 0.9738

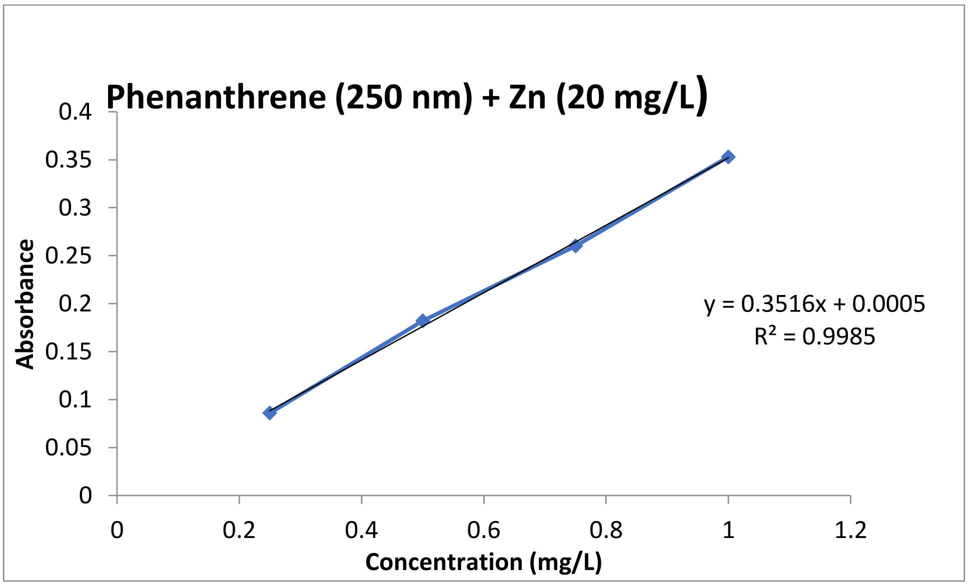
Phenanthrene (250 nm) + Zn (20 mg/L)
Absorbance
Concentration (mg/L)
0.4
0.35
0.3
0.25
0.2
0.15
0.1
0.05
0
0
0.2
0.4
0.6
0.8
1
1.2
y = 0.3516x + 0.0005
R² = 0.9985

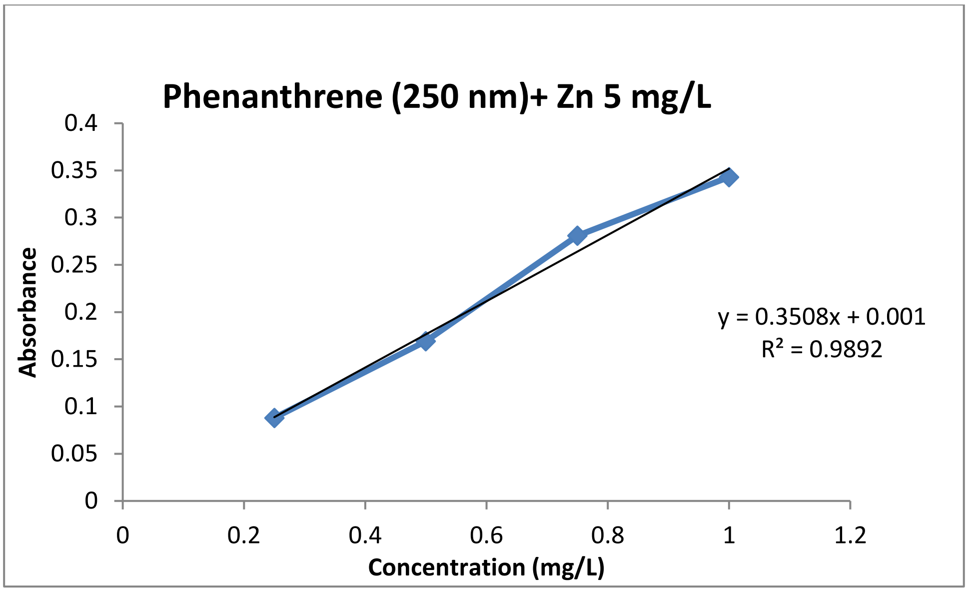
Phenanthrene (250 nm)+ Zn 5 mg/L
Absorbance
0.4
0.35
0.3
0.25
0.2
0.15
0.1
0.05
0
0
0.2
0.4
0.6
0.8
1
1.2
Concentration (mg/L)
y = 0.3508x + 0.001
R² = 0.9892

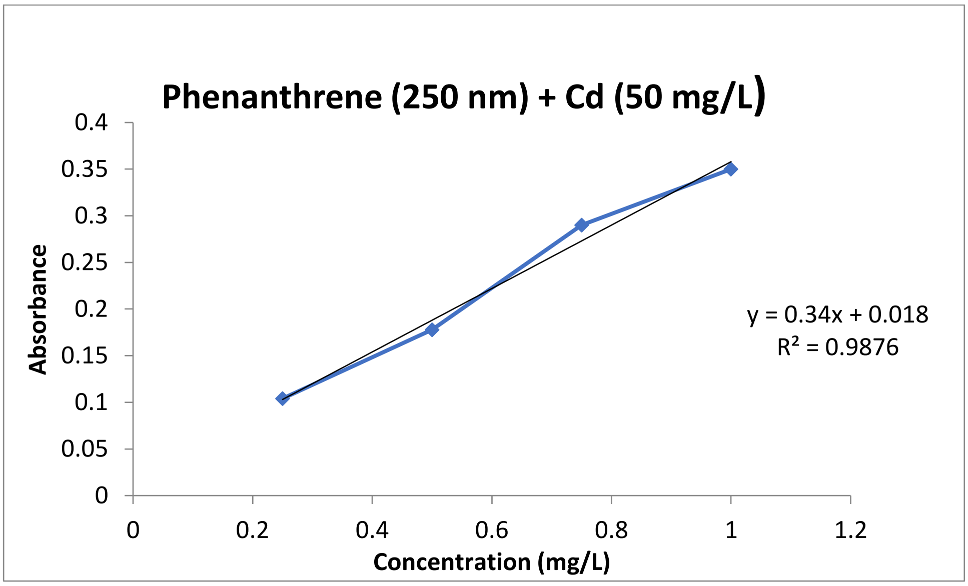
Phenanthrene (250 nm) + Cd (50 mg/L)
Absorbance
0.4
0.35
0.3
0.25
0.2
0.15
0.1
0.05
0
0
0.2
0.4
0.6
0.8
1
1.2
Concentration (mg/L)
y = 0.34x + 0.018
R² = 0.9876

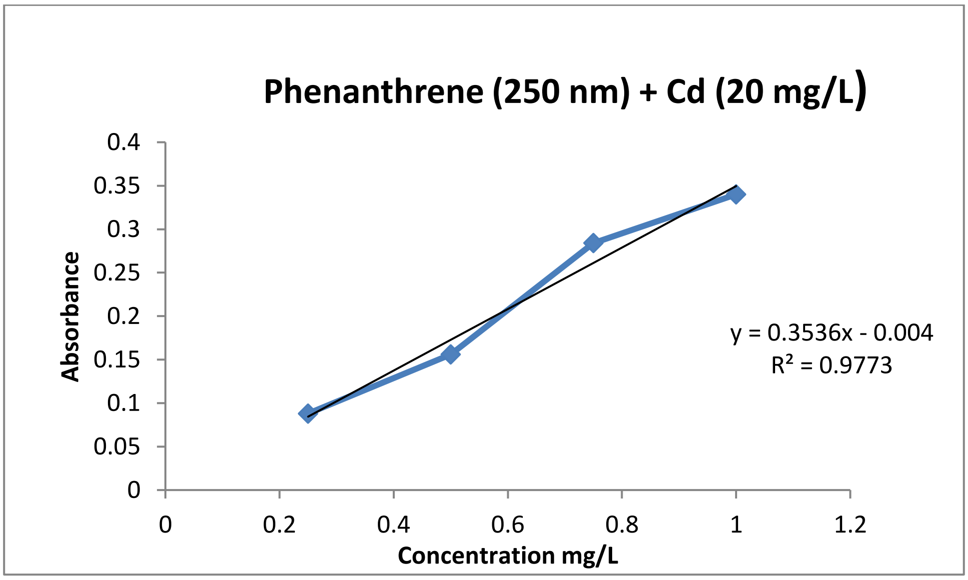
Phenanthrene (250 nm) + Cd (20 mg/L)
Absorbance
0.4
0.35
0.3
0.25
0.2
0.15
0.1
0.05
0
0
0.2
0.4
0.6
0.8
1
1.2
Concentration mg/L
y = 0.3536x - 0.004
R² = 0.9773

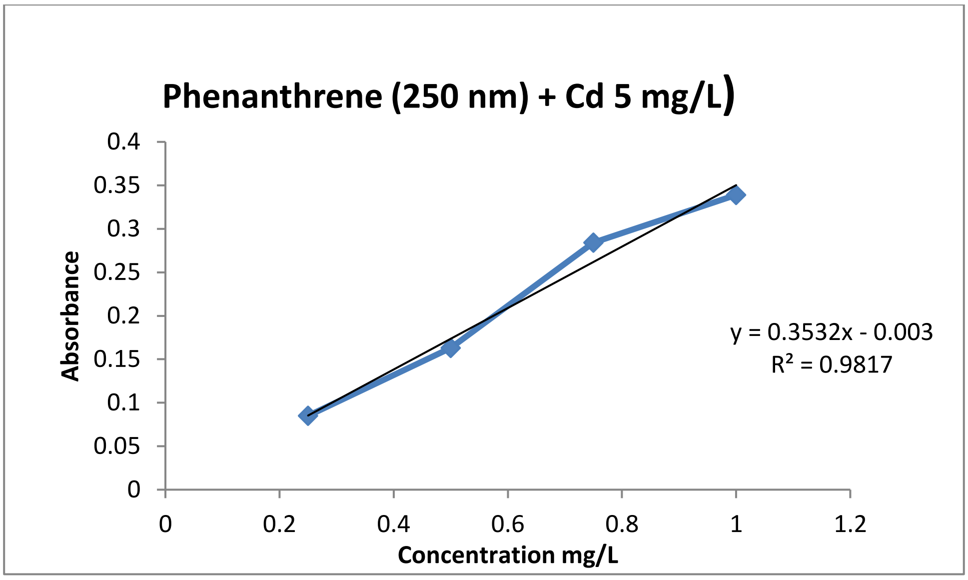

Phenanthrene (250 nm) + Cd 5 mg/L)
Absorbance
0.4
0.35
0.3
0.25
0.2
0.15
0.1
0.05
0
0
0.2
0.4
0.6
0.8
1
1.2
Concentration mg/L
y = 0.3532x - 0.003
R² = 0.9817

Fig. S9: Percentage removal of PAHs (initial concentration 1 mg/L) and metals (initial concentration 5 mg/L)

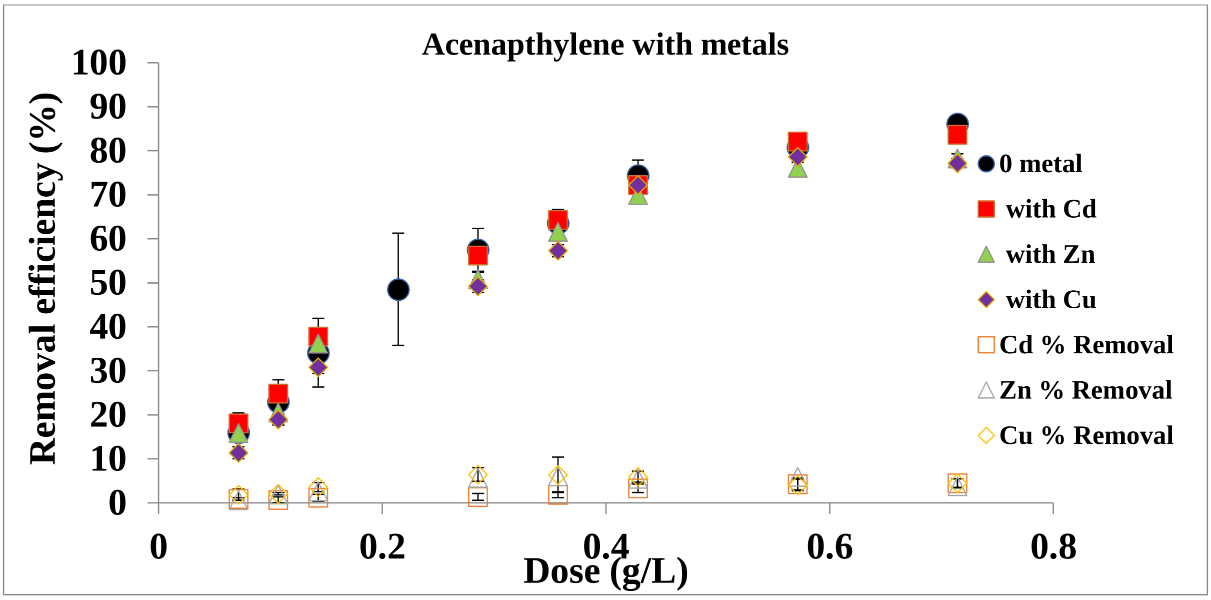

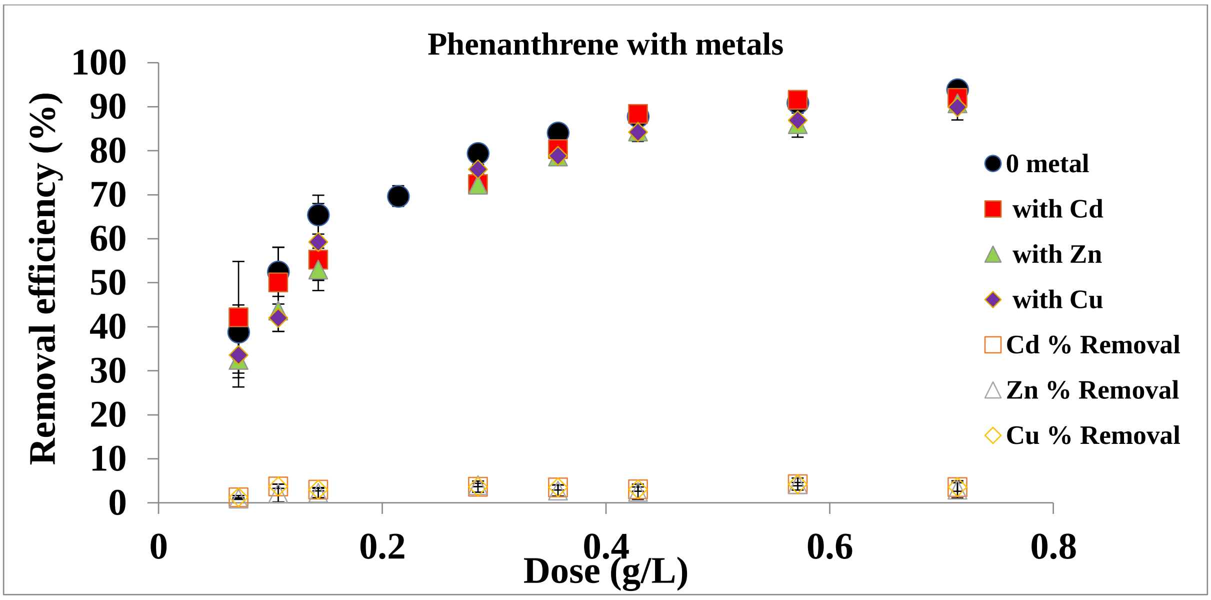

Fig. S10: Amounts of PAHs (initial concentration 1 mg/L) adsorbed in the presence of metals (5 mg/L)

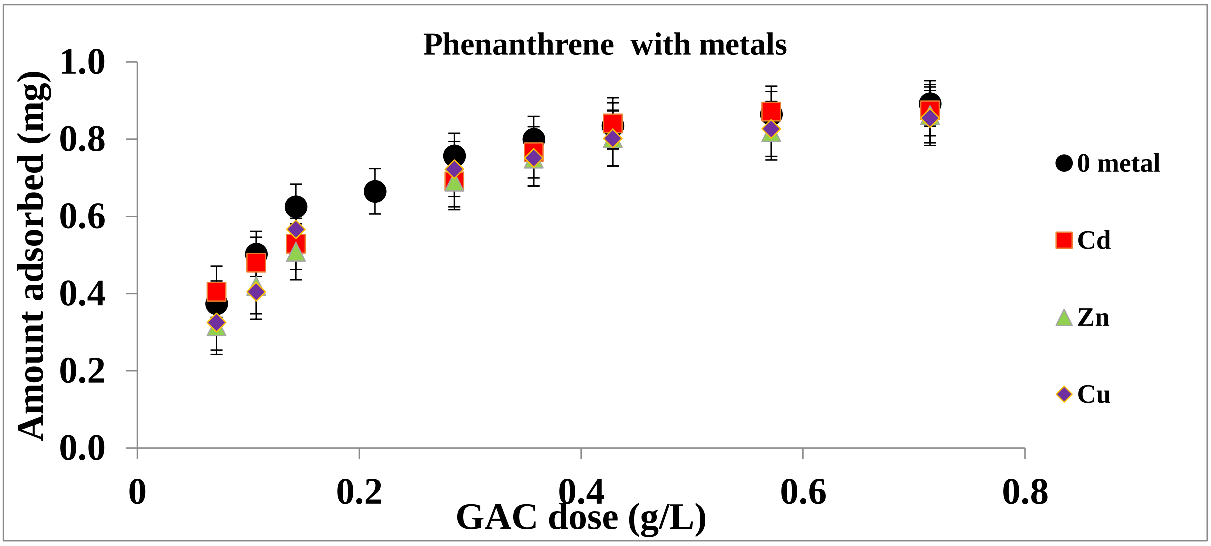

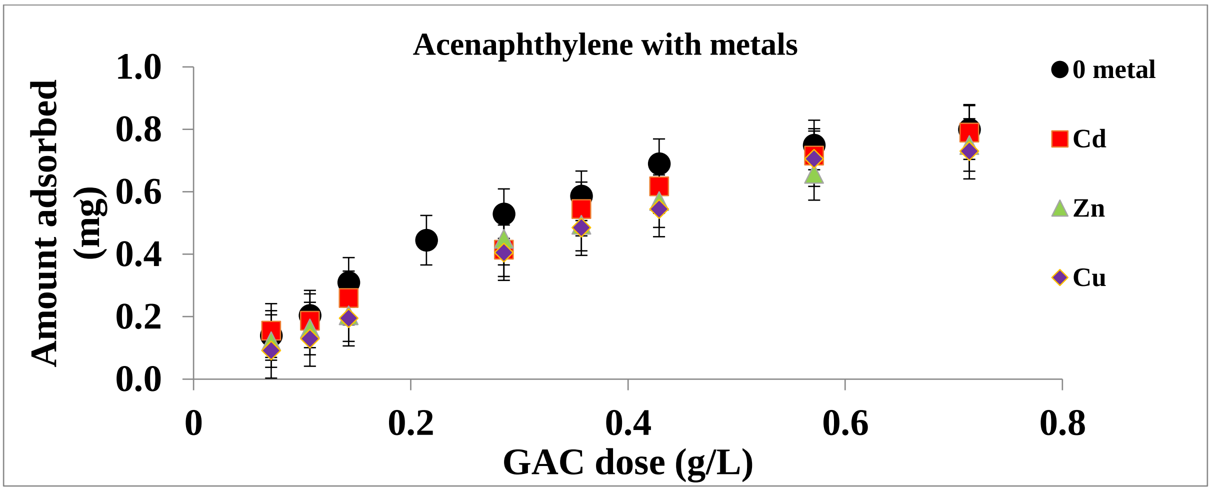

Fig. S11: Amounts of metals (initial concentration 5 mg/L) adsorbed in the presence of PAHs (initial concentration 1 mg/L)